



The Energy Consumption of the Process of Joining Steel Sheets with the Use of Clinching With and Without an Additional Rivet, and Analysis of Sheet Deformation and Mechanical Strength of Joints

Jacek Mucha¹ · Łukasz Boda² · Waldemar Witkowski¹

Received: 12 July 2023 / Revised: 15 February 2024 / Accepted: 20 February 2024
© The Author(s) 2024

Abstract

This paper presents the results of research on the impact of the use of different tools and the shape of the additional rivet, on the geometric quality of the joint, the energy consumption of the forming process, the distortion of the steel samples, and the load capacity of the joints. The tests were carried out for DX51D steel sheets with a thickness of 1.5 [mm] joined by using three different sets of tools. A steel rivet with a hardness of 400HV1 and various shapes was used for the tests. In addition to the full rivet, two types of rivet were used, the first with a through hole and the second with a depth of hole of 3 [mm]. The holes in the rivet had different diameters: 1.0, 1.5, 2.0 and 2.5 [mm]. The influence of changing the shape of the rivet (hole and its diameter) on the change in forming force and energy consumption of the joining process was analyzed. The lowest forming force was achieved for a rivet with a through hole and a hole diameter of 2.5 [mm]. The lowest joint forming force was obtained for the die with movable segments. For joints made with three tool arrangements and a series with a modified rivet, the amount of sheet metal deviation was analyzed. Of the three cases of arrangement of tools used to form the joint, the largest deviation of the sheets occurred at the clinch joint formed with a solid round die. In the case of a series of clinch-rivet joints with a modified rivet, the greatest deviation of the sheets occurred for the rivet with a hole of 1.5 [mm]. Changes in the geometric structure of the joint were also studied, and changes in the surface of the sheets in the joint area were observed. The highest value of the interlock in the joint was obtained when a solid rivet was used in the clinch-riveting technology. The strength of the joints was also identified in the lap shear test and the energy consumption at failure was determined. The use of a rivet increased the maximum load capacity to almost twice that of the clinch joint.

✉ Jacek Mucha
j_mucha@prz.edu.pl

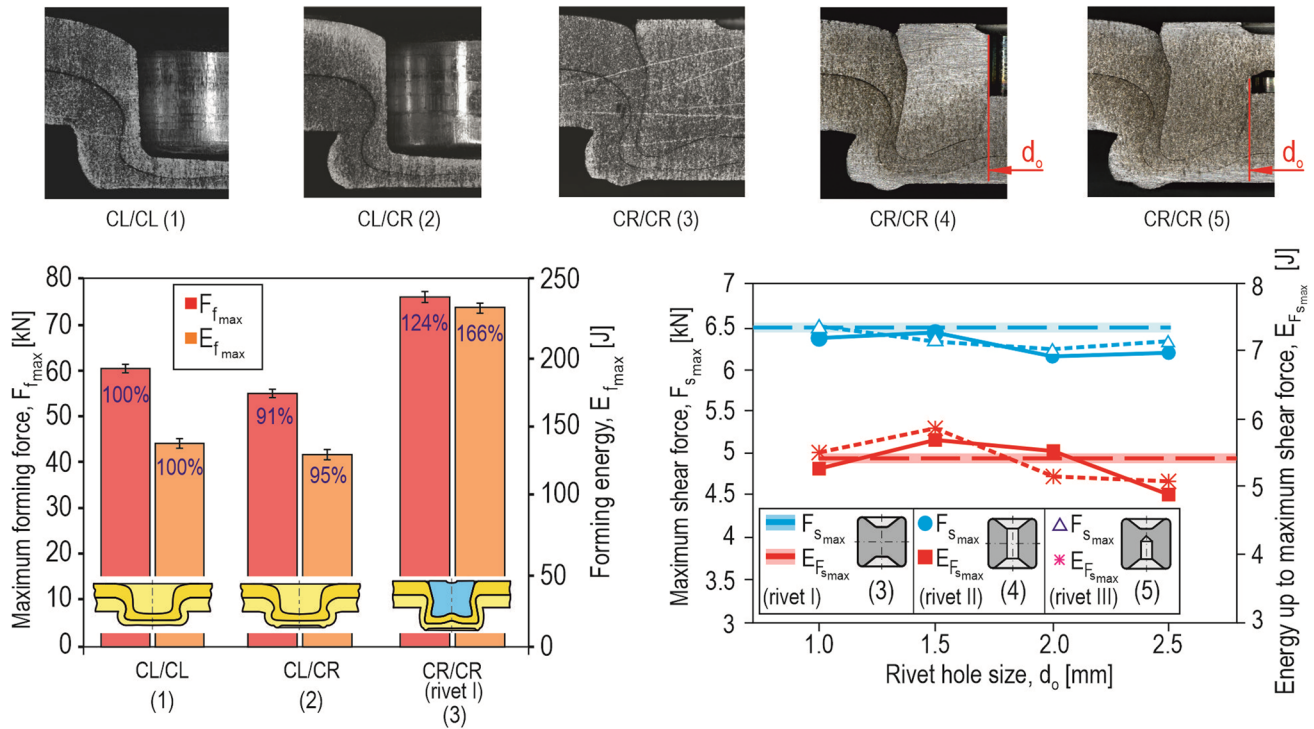
Łukasz Boda
d413@stud.prz.edu.pl

Waldemar Witkowski
wwitkowski@prz.edu.pl

¹ Faculty of Mechanical Engineering and Aeronautics,
Rzeszów University of Technology, al. Powstańców
Warszawy 8, 35-959 Rzeszów, Poland

² Doctoral School of the Rzeszów University of Technology,
Rzeszów University of Technology, al. Powstańców
Warszawy 12, 35-959 Rzeszów, Poland

Graphical abstract



Keywords Clinch joints · Clinch-riveting · Dimensional control · Industry 5.0 · Energy consumption · Rivet modification · Clinch-rivet joints strength

1 Introduction

Automation and computerisation of manufacturing processes (so called “*Industry 5.0*”) is the latest trend in the global industry. In mass production, the assembly lines for the thin-walled elements are equipped with industrial robots (Fig. 1a). The application of a specific joining technology, for plastically formed joints, requires analysis of the maximum forming force and the possibility of mounting a specific set of tools on the C-frame (Fig. 1b). New modifications of joining technologies are being introduced that are characterised by increased joint stiffness and joint strength. However, not all solutions allow to reduce the energy consumption of the process.

Until recently, the most common methods of joining car body elements were techniques based on resistance welding, welding, or laser welding. These processes generate harmful gaseous compounds that affect the purity of the natural environment. A side effect of the above-mentioned processes is, among others, CO₂ emissions. To prevent this, production should take place in tight facilities with internal air circulation and filtration. These installations are expensive. For some time, clinching (“CL”) has been

one of the methods used to join thin-walled structures of vehicles [1, 2]. Clinching is becoming more and more commonly used in the assembly processes of car bodies [3–10]. Sheets of car body structures can be welded with additional adhesive between sheets [11]. The adhesive layer is not a major obstacle in the welding process. The coherence of the material is maintained during the joining process, and there is no material damage of the joined elements. Clinching is also used to join galvanised sheets without significantly damaging the zinc coating [12]. It can replace resistant welded joints in some cases [13]. Clinching technology is constantly being developed and new variations of the clinching process are being developed [14]. One of the modifications of the process concerns the local heating of the materials before joining [15, 16]. It can be used to join when a hole has already been made in the lower layer [17]. Another widely used method of joining without the need to make holes is self-piercing riveting (“SPR”) [18, 19]. However, in the “SPR” joining process, the top layer of the material is pierced. “SPR” can be used to join various materials, including increasingly widely used aluminum alloys [20, 21] and titanium [22, 23]. Another modification of riveting technology without

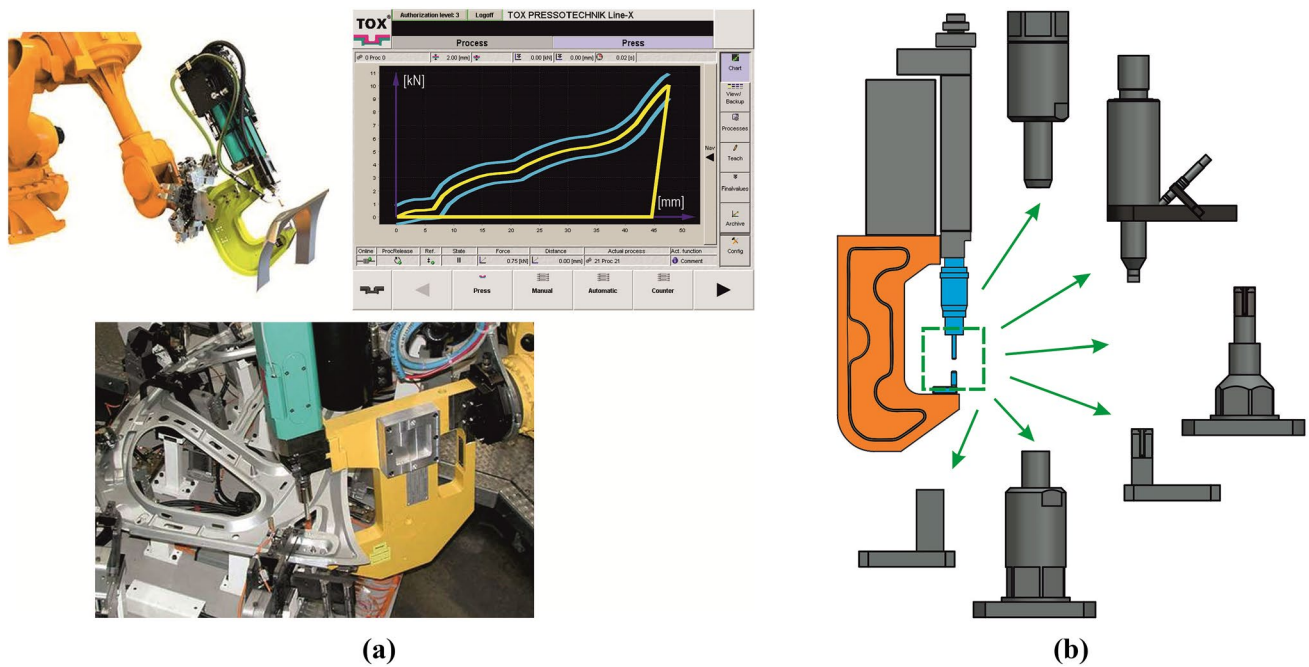


Fig. 1 The industrial robot for joining thin-walled elements with forming force control (a) and the examples of tools used in a C-frame (b)

drilling a hole is joining with a high-hardness rivet, by means of which a hole is punched [24–29]. Another method used to connect the vehicles construction is friction stir welding (“FSW”) [30]. One of the newer modifications of the welding joining process is friction stir spot welds (“FSSW”) [31]. There are no harmful gases in this process. Due to the rotation and contact pressure of the tool, the joined material is heated, which facilitates mixing of the joined sheet material. The process is so innovative that it is constantly being developed and adapted to new applications [32].

In the literature, it can be observed that new types of joint structures are constantly being developed, requiring the development of new types of joining processes [33–36]. Clinching allows for joining steel sheets [37–39], aluminum alloys [40–43] and even titanium alloys [44–47]. The clinching method is constantly developed and modified [48, 49].

In the case of using an additional rivet to form a clinch joint, a significant increase in joint strength is obtained [50]. For all tested joints, the load capacity of the clinch-rivet joint increased several times compared to the clinch joint. However, the forming force required to form the clinch-rivet joint compared to clinching was higher. Another work [51] presented extended research on the joining of clinch-rivet for joining of steel and aluminum alloy sheets. The largest interlock was obtained for the combination of aluminum alloy sheet material. In all cases, the plates were not pierced. Connections made with an additional rivet allow to obtain 93–97% of the load capacity of welded connections for the

same materials [52]. Clinch-riveting can be successfully used to join different types of aluminum alloys with different technological states [53].

The use of a solid rivet modification, i.e. with a through hole, reduces the forming force [54]. The lowest forming force was obtained for a hole with a diameter of 2.5 [mm]. However, no significant reduction was achieved compared to a joint formed without an additional rivet.

The clinch-rivet joints can be formed using a rivet of different hardness. The authors of the paper [55] analysed the influence of different rivet hardnesses (350HV1, 400HV1, 420HV1) on the forming force, interlock parameters, and joint load capacity for a steel sheets.

The use of joining with an additional rivet (without loss of material cohesion) is also possible when using a flat die. This is a way of simplifying the shape of the die. In the paper [56], for a flat die the influence of the sheet holder force on the interlock parameters and joint load capacity for sheets made of aluminum alloy was analysed. It has been shown that the greater the holder force, the greater the interlock parameters and the load capacity of the connection.

A rivet with a hole can be used to regenerate a damaged clinch joint [57–59]. The issue of strengthening a damaged joint made of sheets of aluminum alloy with a tubular rivet made aluminum alloy is presented in [57]. After placing the tubular rivet, the joint was pressed with varying force. A flat die was used in the experiment. A similar method for strengthening a damaged clinch joint was presented in [58, 59]. The reinforced connection showed a higher load

capacity than the undamaged clinching connection without the rivet. The paper [60] presents research on joining with the use of a solid rivet and a hole rivet in a two-stage forming process. However, this requires a more complex forming process, so the costs are higher and the assembly time is longer. They obtained a significant increase in the size of the interlock and the load capacity of the joint. The results of the optimisation related to the location of the special groove on the cylindrical surface of the solid rivet and the impact on the load capacity of the connection are presented in the paper [61]. In this case, the full rivet was also made of steel with a hardness of 62 HRC. A flat die and a slotted holder were used for joint forming.

Each of the methods of joining thin-walled structures causes, to a greater or lesser extent, deviations of the material in the vicinity of the joint axis. During joining, in addition to local changes in the structure of the material, there is a specific deviation of the surface of the sheets (Fig. 2a). Examples of deformations of thin-walled elements are shown in Fig. 2b.

One of the most interesting paper about the deformation of joined sheets using “SPR” technology is the publication by Cai et al. [62]. The issue of predicting the surface deviation of the joined aluminum alloy elements with the use of “SPR” joining technology was analysed by Cai et al. [63]. During the research, they analysed the effect of the length of the rivet on the joining process parameters and deformation of the aluminum alloy sheets. In addition, for a specific aluminum alloy door panel, an algorithm was applied to predict the deformation of specific surfaces. Tozaki et al. [64] studied the behaviour of joined materials in the structure and deformations around the joint. For various shapes of the tool and the technological parameters of the friction stir welding process, they performed an analysis of the microstructure

and load capacity of the lap joint of aluminum alloy sheets. Friction stir welding causes an increase in temperature at the connection point, which affects changes in the material and thermal deformations [65]. Hwang et al. [65] investigated the influence of technological parameters of friction stir welding on the range of temperature impact in the joined materials.

Often, in addition to joining thin-walled layers of the structure, it is necessary to form an additional thread in a specific place. This effect can be achieved by mechanical locking pressing of additional fasteners [66, 67]. In the papers [66, 67], the authors present the analysis of the load capacity of a joint with a plastically clamped additional element with a thread. They proposed a variant of the connection technology in which there is already a flange in the material and that is used to tighten the threaded fastener.

In [68], the authors presented research on the assembly of a special threaded element using friction stud riveting (“FSR”). “FSR” causes the material to deform plastically and thermally around the injection place. A flash of material is formed around the pressed in additional element, which may affect the adhesion of the joined elements. Mechanical clamping of additional elements allows you to quickly create a place with a thread. The thread allows for the assembly of a separable connection.

This paper presents research, results, and their analysis regarding the possibility of using a modified steel deformable rivet with a hardness of 400HV1 as an additional element for forming a clinch joint. To form the clinching connection with an additional rivet, a full rivet was used, a rivet with a through hole, and a rivet with hole depth of 3.0 [mm] were used. To compare the effect of using an additional rivet, the clinch joint was formed without a rivet using a rigid circular die and a die with movable segments. Furthermore,

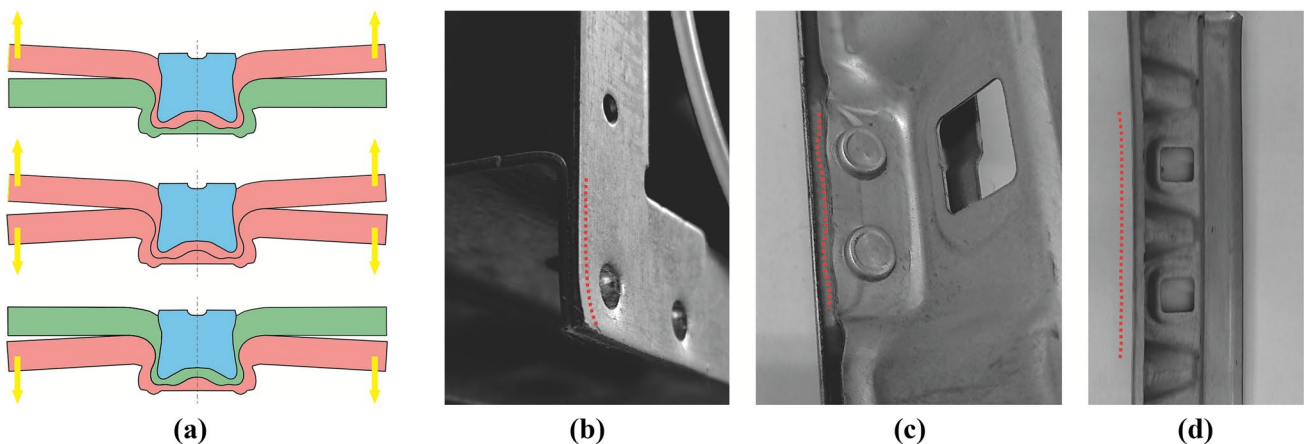


Fig. 2 Basic examples of the deformation of the sheets with a clinch-rivet joints—(a), examples of deformation of the sheet surfaces with the clinch joint for: steel sheets—(b, c), aluminium alloy sheets—(d)

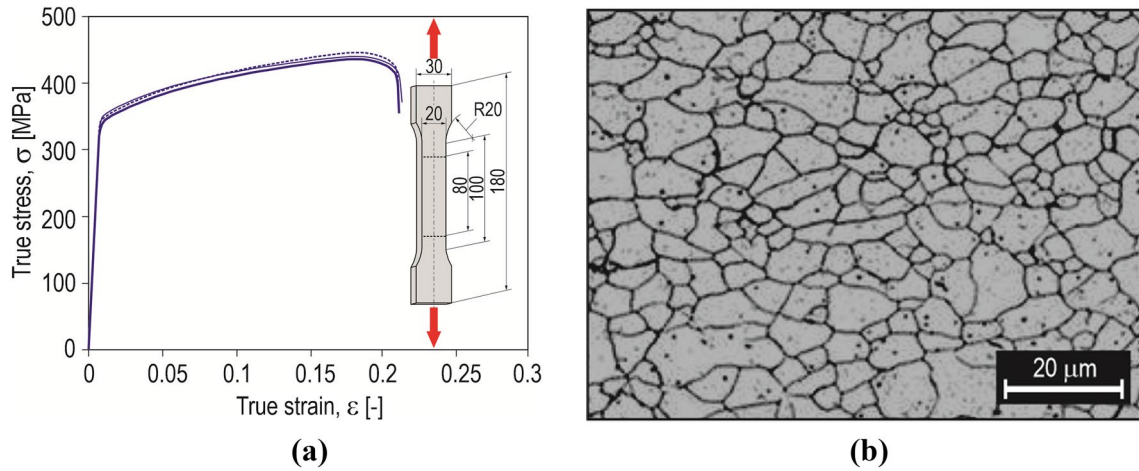


Fig. 3 DX51D sheet material characteristic: **a** true stress-true strain curve (according to [70]), **b** microstructure

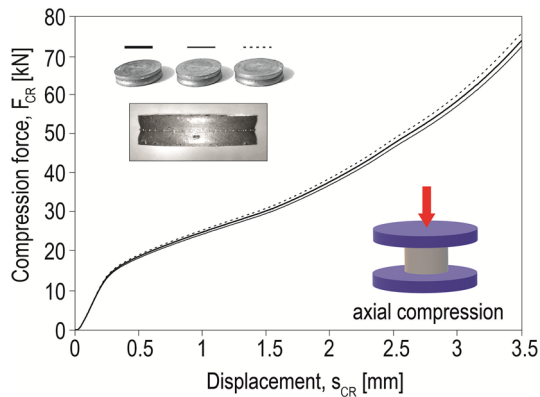


Fig. 4 Examples of the force–displacement diagrams obtained in the upsetting test of the rivets

an analysis of the energy consumption of the forming process was made for different variants of tools and the shape of the rivet. The basic geometry of the interlock on the

cross-section of the joints and the deformation of the samples were measured. The load capacity of the lap joints was also tested for a DX51D steel sheets of 1.5 [mm] thickness with a ZnNc coating.

2 Methodology for Measuring Sheet Deviations and Load Capacity of Joints Formed with Different Sets of Tools

A DX51D+Z/275 (according to PN-EN 10346: 2015-09 [69], material number 1.0917) steel sheet with a thickness of 1.5 ± 0.15 [mm] with a ZnNc coating was used to test the clinch joints formation process. The true stress-true strain diagram of the sheet material, according to PN -EN ISO 6892-1:2020-05 [70], is shown in Fig. 3a. The microstructure of the steel was identified on the etched specimen (Fig. 3b).

The standard and modified rivets used in the experimental tests are made of carbon steel with 205 [GPa] Young's

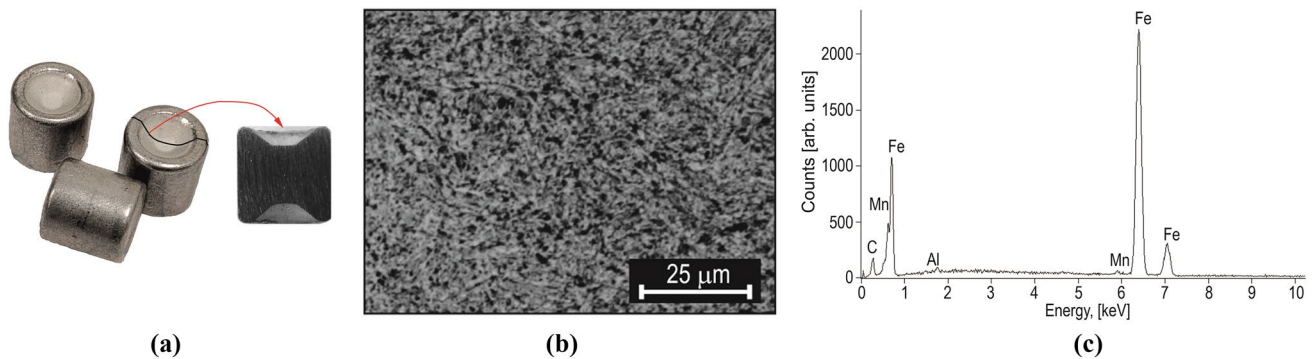


Fig. 5 View of the rivet and its axial section—**a**, rivet microstructure—**(b)**, EDS spectrum of steel particle—**(c)**

modulus (E), 0.3 Poisson's ratio (ν), and 400HV1 hardness. Microhardness measurement was performed in accordance with the PN-EN ISO 6507-1:2018-05 standard [71]. The compression force–displacement diagrams in the rivet upsetting tests are shown in Fig. 4. In the cross section of the solid rivet (Fig. 5a), the macrostructure of the rivet material was observed (Fig. 5b). The identification of the material by analysing the chemical composition in microareas was performed by using the Hitachi S-3400N scanning electron microscope, which uses X-ray energy dispersion spectroscopy (“EDS”), according to the ASTM E-1508-12 standard [72]. An accelerating voltage of 20 [kV] and a spot size < 10 [nm] were used. A backscattered electron (“BSE”) detector was used. The obtained X-ray spectra is shown in Fig. 5c.

The tests of forming process of all joints, including three variants of the rivet geometry, were performed in the Pressed Joint Laboratory of the Machine Design Department at Rzeszow University of Technology. The stand enables the formation of various plastically shaped joints up to 100 [kN]. The “CMB” C-frame press was equipped with an EMPK linear servo drive, force measurement systems with an accuracy of 0.5% of the pressing force, and the displacement measurement with an accuracy of 0.01 [mm]. The stand has interchangeable sets of forming tools for 3 types of joints (Fig. 6a):

1. Clinching—round punch and solid die (“CL/CL”).
2. Clinching—round punch and die with movable segments (“CL/CR”).
3. Clinch-riveting—rivet feeder punch, deformable full rivet and “SKB” die with movable segments (“CR/CR”).

The detailed geometry and arrangements of the forming tools are included in Fig. 6b. In addition, three variants of the rivet geometry were used for the tests (Fig. 7). Based on

the standard rivet geometry (Fig. 7a), a specific modifications were made: hole with a certain depth (Fig. 7b) and through hole (Fig. 7c). The individual nomenclature of the joints is listed in Table 1.

In the case of modification of the rivet geometry, a reduction in the weight of the rivet was obtained. The largest decrease was obtained for the diameter of the 2.5 [mm] through hole. For individual variants of the rivet shape, individual weight change parameters were measured and calculated, which are listed in Table 2. In the case of forming clinch joints without a rivet, a punch with a diameter of $d=5$ [mm] was used (Fig. 6b). In the case of joints with an additional rivet, a rivet of the same diameter as the forming punch (“CL”) was used—Figs. 6b and 7. For joints without a rivet, the thickness of the embossment was set at $X=0.75$ [mm], and for joints formed with a deformable rivet the zero distance between the upper surface of the rivet and the upper surface of the upper sheet was set (Fig. 8).

For all variants of the joints, observations and measurements of the characteristic parameters of the joints interlocks were made (Fig. 9). Observations and measurements of the joint geometry were made using the VHX7000 optical

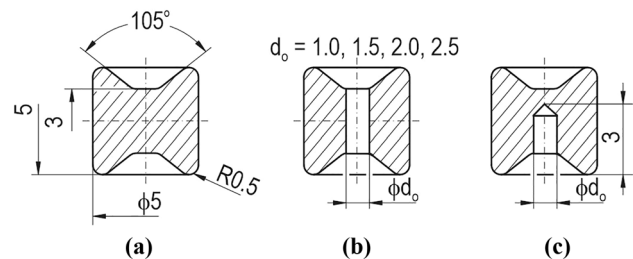


Fig. 7 The variants of the shape and geometry of the rivets used in test: **a** full rivet (rivet I), **b** rivet with through hole (rivet II), **c** rivet with a hole depth of 3 [mm] (rivet III); the dimensions in [mm]

Fig. 6 The joint forming stand: **a** stationary C-frame press (5), **b** tools dimension and their arrangement scheme (1—clinching-riveting punch system, 2—die with movable segments, 3—clinching punch, 4—clinching die)

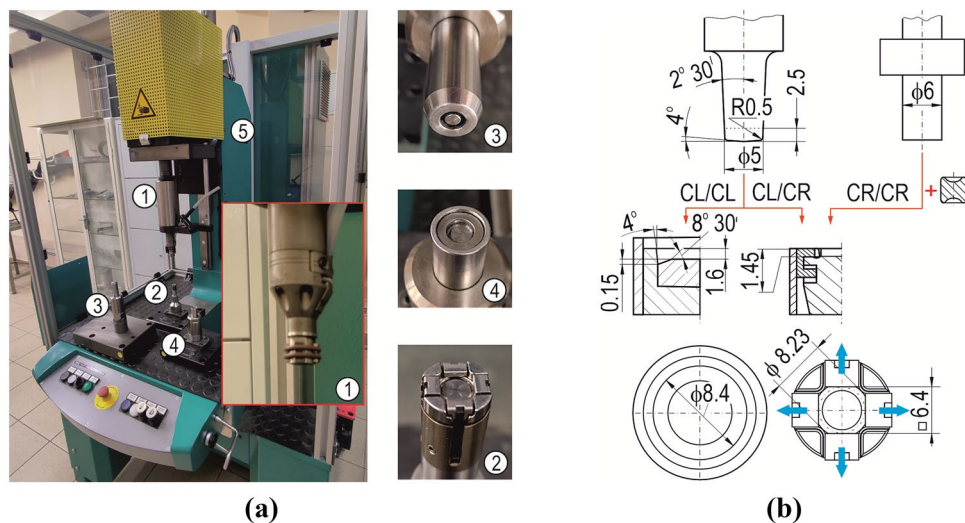


Table 1 The tools and an additional elements arrangements

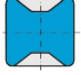
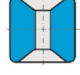
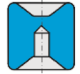
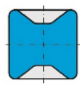
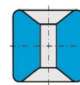
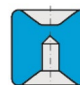
Punch type	“CL”		“CR”						
Die type	“CL”	“CR”	“CR”						
			Rivet hole, d_o [mm]						
			0	Hole type	1.0	1.5	2.0	2.5	
Additional element	–	–	Rivet I 	Rivet II 	“CR/CR1.0”	“CR/CR1.5”	“CR/CR2.0”	“CR/CR2.5”	
Nomenclature	“CL/CL”	“CL/CR”	“CR/CR”	Rivet III 	“CR/CR-1.0”	“CR/CR-1.5”	“CR/CR-2.0”	“CR/CR-2.5”	

Table 2 The weights comparison of the full rivet and rivets with holes

Parameter	The geometrical shape of the rivet hole									
	Rivet I 	Rivet II 				Rivet III 				
Diameter of the rivet hole, d_o [mm]	0	1.0	1.5	2.0	2.5	1.0	1.5	2.0	2.5	
Rivet weight, g_r [g]	0.678	0.660	0.636	0.599	0.546	0.667	0.654	0.636	0.612	
Rivet relative weight to a full rivet, u [%]	100	97.35	93.81	88.35	80.53	98.37	96.46	93.80	90.26	
Weight change, Δg_r [%]	0	2.65	6.19	11.65	19.46	1.63	3.54	6.20	9.74	

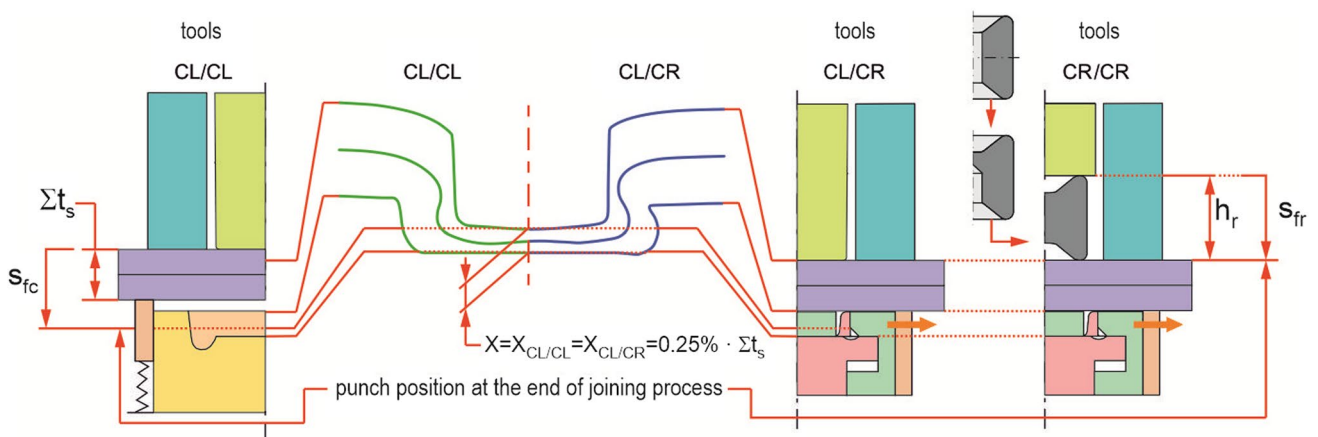


Fig. 8 The final position of forming tools for “CL/CR” method (left side), “CR/CR” method (right side). s_{fr} —punch displacement, h_r —rivet height, X —minimal thickness of the embossment, Σt_s —total sheets thicknesses, s_{fc} —displacement for joints without rivet

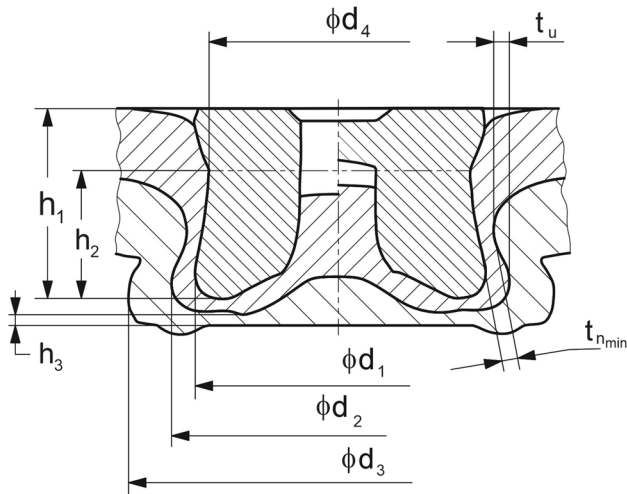


Fig. 9 The interlock parameters of the clinch-rivet joint

microscope. The microscope was equipped with a VH-Z20R/Z20T zoom lens. The parameters were analysed for a zoom of 100 \times , which allowed one to obtain a single image with a resolution of 2048 \times 1536 [px] with a working area of 3.05 [mm] by 2.28 [mm]. The lens distance was 25.5 mm. The distance between the pixels of the recorded image was 0.0015 [mm], in both directions of the XY plane.

Identification of the size of the sheets deviation from the initial position was carried out by measuring the deviations of the outer surfaces of the sheets of the sample with dimensions as in Fig. 10a. On the other hand, to test the joint load capacity and the energy consumption, lap joints samples were prepared with various arrangements of the forming tools and the rivet geometry (Fig. 10b). The lap joints for the shear tests were made in accordance with the ISO 12996:2013 standard [73].

In the case of measuring the deviation of the sheets, the origin of the axis system was adopted on the sheet surface—Fig. 11. In order to increase the accuracy of the measurement

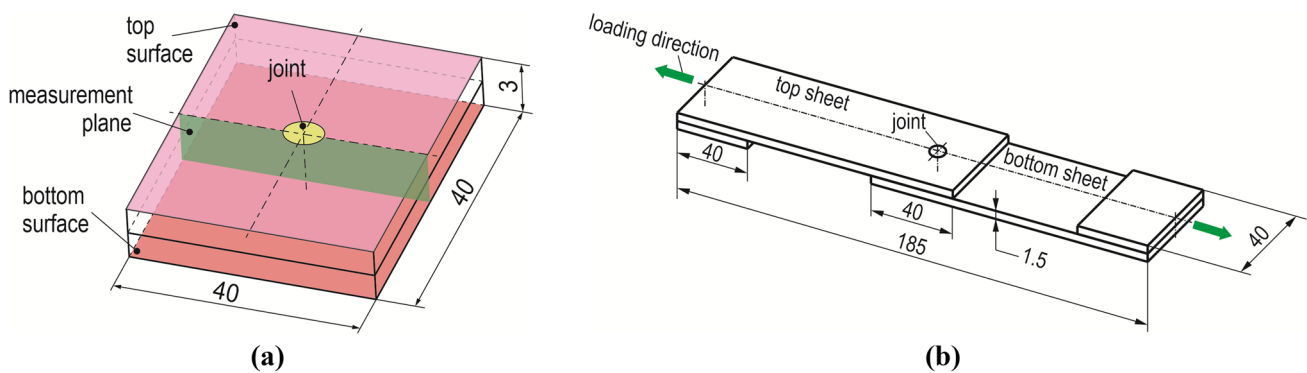


Fig. 10 The dimensions (in [mm]) of the sheet samples for: **a** sheet deviations measurements, **b** joint strength tests

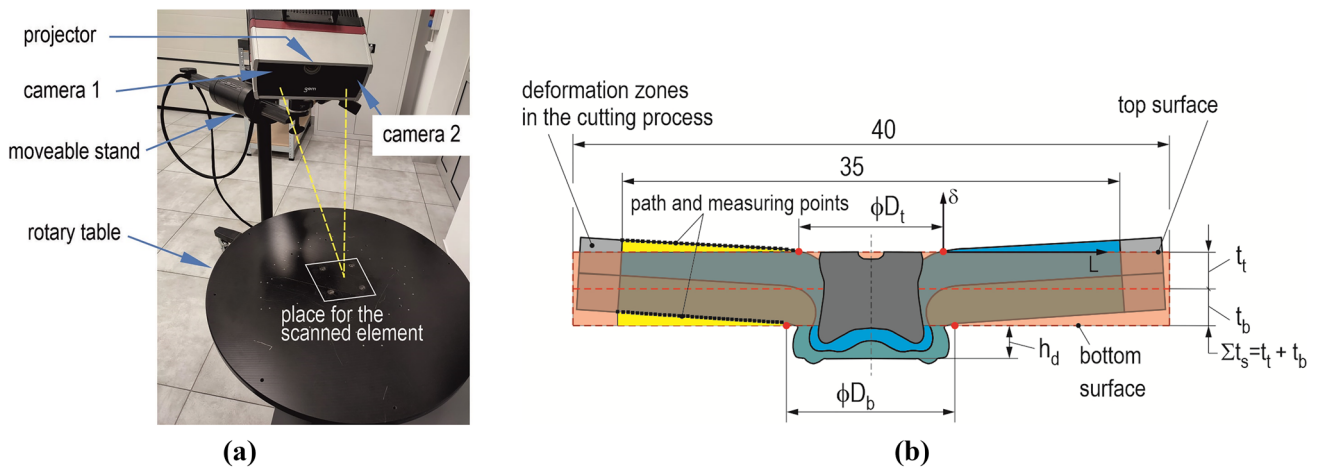


Fig. 11 The measuring apparatus—(a), characteristics of the method of the sheet deviations measurements—(b)

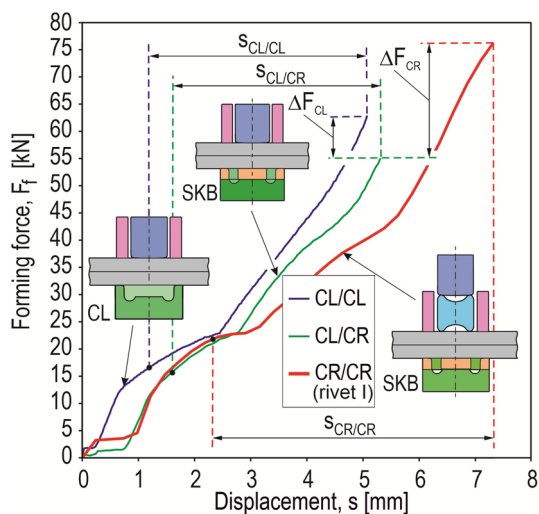


Fig. 12 The examples of the forming force–displacement diagrams for different tools arrangement

of the sheet edge deviation line, the part deformed as a result of samples preparing (cutting process) was omitted. On the press, during the strip cutting process, the sheets were pressed down with a holder. The size of the sheet surface deviations was measured with the ATOS Capsule 200 MV200 scanner (Fig. 11a). The measurement system was characterised by the maximum measurement error: sphere spacing error 0.008 [mm] and length measurement error: 0.009 [mm]. After the scan, points were set along the path shown in Fig. 11b.

3 Results and Discussion

Changing the type of joining technology for one sheet layout arrangement affects the energy consumption, interlock geometry, and load capacity of pressed joints. It is possible to use different sets of tools for one C-frame stand. “CR” technology requires a frame with more clearance than a rivetless joint forming tool kit. The rivet feeder system with a punch and a rivet feeding mechanism has much larger dimensions than the punch holder for clinch joints [54]. In the case of the manipulator, the weight of the tools is important. “CL” technology allows the use of a rigid tool and a relatively simple solid die, but no significant load capacity of the sheet joint is achieved. The use of a matrix with movable segments allows to reduce the energy consumption of the joining process. The use of an additional deformable element (rivet) significantly changes the forming process and the maximum load capacity of the joint [60]. For selected variants of the forming process, the size of the deviation of the joined sheets was measured. The influence of the die

used in the clinch joint formation process on the maximum load capacity of the lap joint was also analysed.

3.1 Analysis of the Energy Consumption of the Forming Processes

An important role in the process of forming clinch joints is the pressure on the joined sheets, hence the holder springs are used in the punch system [56]. Sometimes there is a blockage of the joint embossment in the die after forming, which is why die ejector systems are used (additional spring in die system). There are many publications in which the authors present an analysis of the formation of pressed joints, but omit aspects of energy consumption of the joining technology. Figure 12 shows the forming force–displacement curves, taking into account the holder spring force, obtained during the formation process. The use of other die than solid, e.g. “SKB” (with movable segments), allowed to reduce the forming force and energy consumption (Fig. 13). It is possible to form a joint with or without an additional rivet (as a classic clinching process) and with a round die with movable segments [44, 58]. A significant increase in the load capacity of the joint can also be achieved by using a rivet and welding it using the hybrid clinching-welding process [15]. However, in this case, the process is more complicated and harmful gases are produced.

The use of an additional solid rivet resulted in an increase in the forming force and the energy consumption of the joining process. The stiffness of the C-frame press for forming clinch joints is extremely important [74]. Hence, it is extremely important to look for possibilities to increase the load capacity of the clinch joint, but not to increase the forming force [54]. It is possible to press the rivet directly into the joined sheets and into the already formed joint [60].

An important role in the process of forming clinch joints is the pressure on the joined sheets, hence the holder springs are used in the punch system. Sometimes there is a blockage

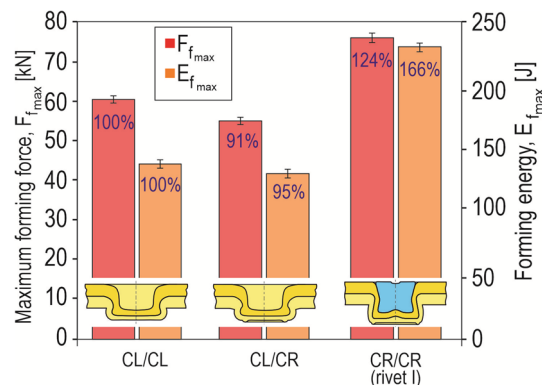


Fig. 13 The comparison of the average values of the forming force and energy consumption for different joining technologies

of the joint embossment in the die after forming, which is why die ejector systems are used (additional spring in die system). There are many publications in which the authors present an analysis of the formation of pressed joints, but omit aspects of energy consumption of the joining technology [75]. Figure 12 shows the forming force–displacement curves, taking into account the holder spring force, obtained during the formation process. The use of other die than solid, e.g. “SKB” (with movable segments), allowed to reduce the forming force and energy consumption (Fig. 13). It is possible to form a joint with an additional rivet and a die with movable segments [60]. The use of an additional solid rivet resulted in an increase in the forming force and the energy consumption of the joining process. The stiffness of the C-frame press for forming clinch joints is extremely important [74]. Hence, it is extremely important to look for possibilities to increase the load capacity of the clinch joint, but not to increase the forming force [54].

The idea of using an additional rivet is to increase the load capacity of the joint. Therefore, it was decided to investigate how modification of the shape (and thus also weight) of the rivet will influence the maximum forming force and energy consumption of the joining process. Figure 14 shows the forming force–displacement diagrams of joint with an additional rivet. The lowest forming force (F_{fmin}) was obtained for “CR/CR2.5” joint with the rivet of 2.5 [mm] hole diameter. The highest value of forming force (F_{fmax}) was obtained in the case of rivet I. The shape of the modified one (with a hole made in the axis to a depth of 3.0 [mm]) looks like a rivet for self-piercing riveting (“SPR”). The difference in the process is significant, in the case of “SPR” the rivet pierces the upper layers of the sheets [18], while in the case of “CR” there is no loss of material cohesion [50]. Modifying the geometry of the rivet allowed for a significant reduction in the forming force, and the course of the forming curve also changed (Fig. 14). In all cases of modification of the rivet

Fig. 14 The forming force–displacement diagrams for joint with rivet and without hole (d_o in [mm])

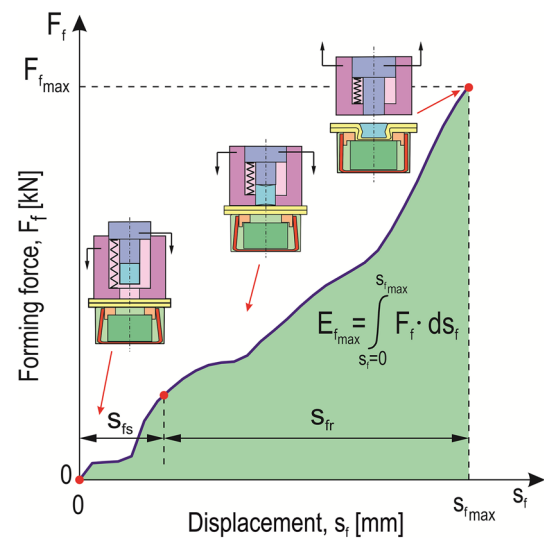
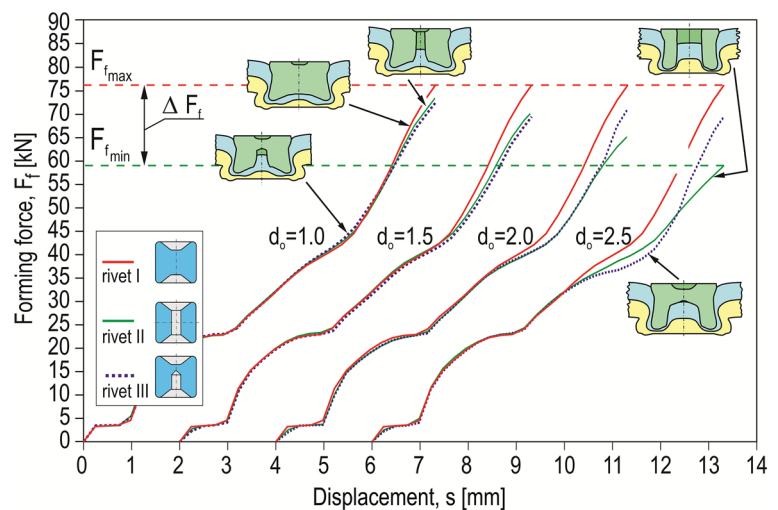


Fig. 15 Forming force–displacement diagram and forming energy of the clinch-rivet joint (s_{fs} —displacement resulting from deflection of the tool springs, s_{fr} —displacement resulting from the pressing of the rivet)

geometry, the energy consumption of the forming process was higher compared to the formation of a connection with a round solid die (Fig. 13).

Based on the forming force–displacement diagrams, the forming energy was calculated (Fig. 15). For two different cases of the shape of the rivet with a hole, a comparison of the maximum forming force and energy consumption of the clinch-rivet joint was made (Fig. 16). In the case of the rivet with a hole of 1.0 and 1.5 [mm], no significant differences were observed. Tests have shown that the use of a rivet with a 2.0 [mm] diameter through hole significantly reduces both the forming force and energy consumption. The differences between the forming force and the energy consumption for the two varieties of the hole in the rivet are at a similar

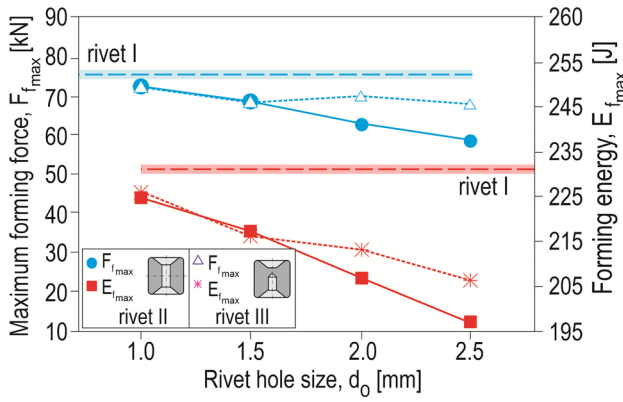


Fig. 16 The influence of the diameter of the rivet hole on the forming force and energy consumption

level. The mechanical characteristics of the rivet influence the reduction of the forming force–displacement diagram course and the increase of the maximum force [55]. Another method, in addition to modifying the tools and the geometry of the rivet, is the use of local heating of the joined sheets [44]. However, this causes thermal and mechanical changes in the joined materials.

3.2 Macrostructure and Measurements of the Joint Interlock Parameters

The formation of the joint with a punch and a solid die is characterised by a limited flow of the material. The shape and geometry of the die used in the forming process influence the mechanism of material flow [76]. The use of a die with movable segments (instead of a solid die) resulted in a greater displacement of the material in the radial direction, especially in the segment area (Fig. 17). Thus, the interlock parameters increased (Fig. 18).

The formation of the joint with a punch and a solid die is characterised by a limited flow of the material. The shape and geometry of the die used in the forming process

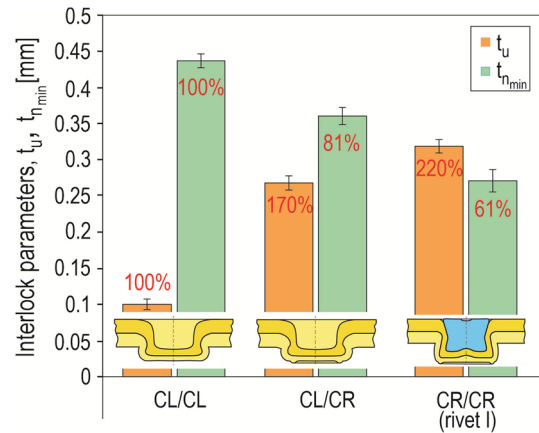


Fig. 18 The interlock parameters for different joining technologies

influence the mechanism of material flow [57, 76]. The use of a die with movable segments (instead of a solid die) resulted in a greater displacement of the material in the radial direction, especially in the segment area (Fig. 17). Thus, the interlock parameters increased (Fig. 18). Dies with movable segments are more complicated than solid dies. It is possible to completely simplify their construction to a flat surface [48]. However, the process of forming such technology for materials available on the market has not yet been well-studied. When joining micro-thick materials, to avoid material cracking, local heating can be used, with the use of a laser beam, of the upper layer of the material pressed into the already punched hole [77].

As the diameter of the hole in rivet II increased, the sheet material under the rivet was pushed into the hole. Thus, the sheet material is pressing on the side surface of the rivet. In a joint with a rivet II and a diameter of 2.5 [mm], the rivet had a similar radius of the inner and outer walls (Fig. 19a—detail No. 1). The rivet was pressed to a greater extent in the direction of its insertion. In the case of a rivet with a hole with a diameter of 1.0 [mm], there was a part of the conical surface of the countersink (Fig. 19a—detail 2). The

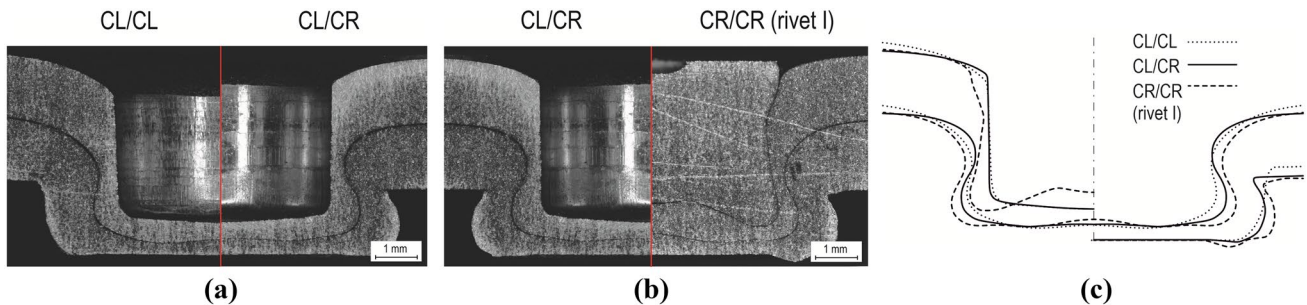


Fig. 17 The comparison of the macrostructure of the joint: **a** formed by using solid die and die with movable segments, **b** formed by using punch, an additional rivet, and die with movable segments, **c** the outlines of the upper (left view) and lower (right view) sheet

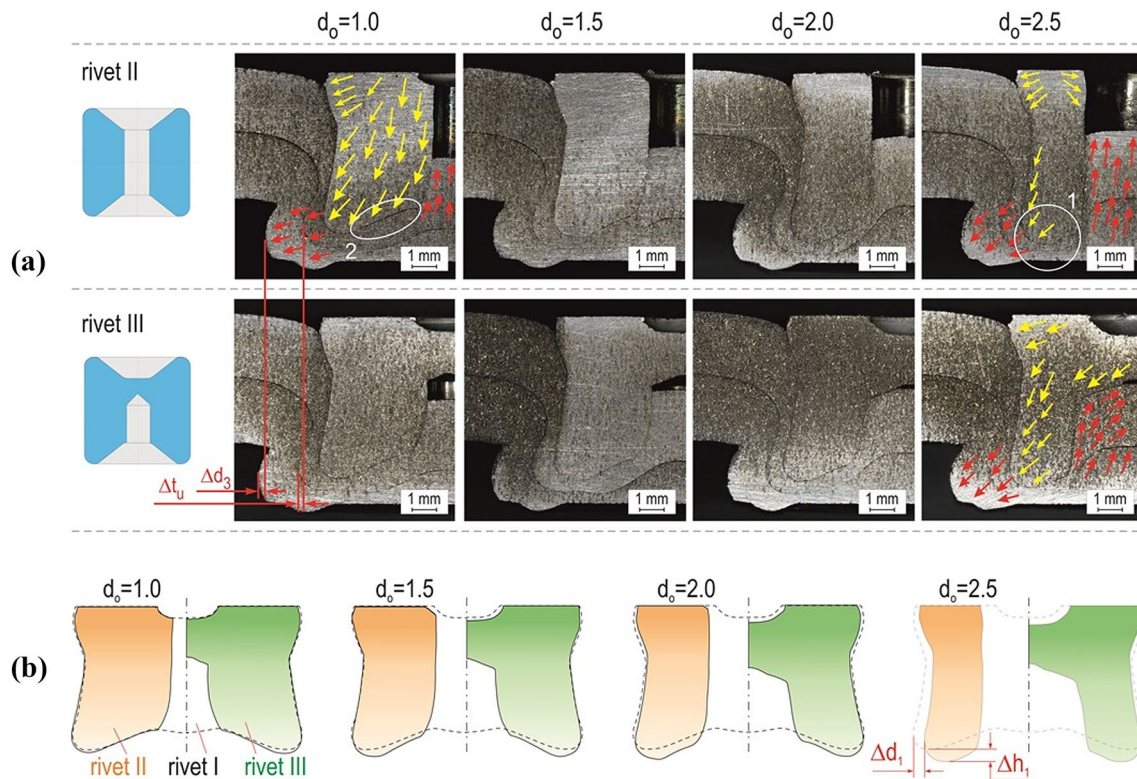


Fig. 19 The macrostructure of the clinch-rivet joints formed with different diameters of the rivet hole—(a), the comparison of the rivet outline for rivets with through hole and 3 [mm] depth hole (solid lines)—background is a full rivet (dashed line)—(b) (d_o in [mm])

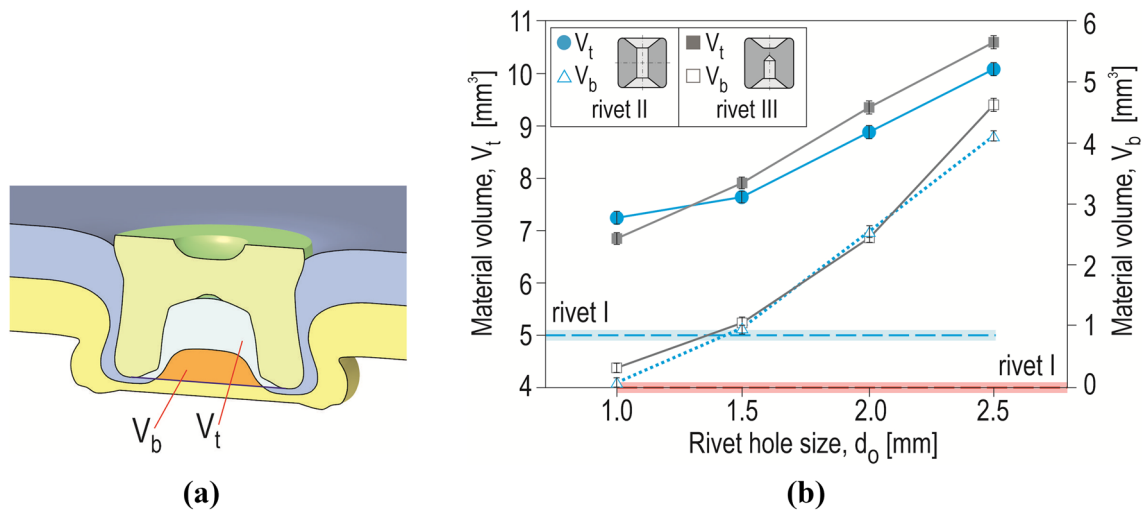


Fig. 20 The upper and lower sheet material in the rivet hole—(a) and the influence of the rivet type on the changes in the volume of the sheet material in the rivet hole—(b)

differences between the height and shape of rivets II and III compared to rivet I are shown in Fig. 19b. The greatest difference in the depth (Δh_1) rivets II and III in sheets was obtained for the diameter of the hole of 2.5 [mm], and the highest radial rivet high in the upper sheet for a rivet with

a hole of 1.0 [mm]. In the case of rivet II, the difference in radial displacement (Δd_1) on diameter d_1 was greater than for rivet III. A rivet with a thinner wall pressed the joined sheet materials to a greater extent (up to 2.5 [mm]). Therefore, a larger volume of material was pushed into the hole in

the transverse directions of the rivet (Fig. 20). For all joints, there was no material cohesion loss of the upper sheet. The issue of pressing an additional deformable aluminum alloy rivet, during which the upper sheet is pierced, was presented in [78]. Piercing of the upper sheets occurs in the case of self-piercing riveting [18, 79], or in another joining method such as shear clinching [80]. When using a rivet with a hole of 1.5 [mm], an improvement in material flow into the free space of the rivet hole was observed. The larger the diameter of the hole in the rivet, the greater the material volume of the upper (V_u) and lower (V_b) sheets was—Fig. 20b. The principle of measuring the volume of material under the rivet is shown in Fig. 20a. In the case of the rivet III, the change in the volume of the upper sheet material (V_u) under the rivet was proportional. The material flow outside the rivet and inside the rivet hole is influenced by the forming force (Fig. 14) and the joint macrostructure (Fig. 18a).

After measurements on the microscope and the recording results, charts of the relationship between the impact of the diameter and shape of the hole on the change in the size of the interlock t_u (Fig. 21a) and the neck thickness ($t_{n_{min}}$) were made (Fig. 21b). Compared to the joint with a solid rivet for a diameter of the rivet hole of 1.0 [mm] (“CR/CR1.0”), a value of t_u decreases about 3.12%. In the case of a rivet with a through hole and diameter from 1.0 to 2.0 [mm], no difference in the size of the interlock t_u was observed. The use of a rivet with a hole diameter of 2.5 [mm] (“CR/CR2.5”) resulted in a decrease in size t_u by 9.68% compared to the joint with a rivet with a hole diameter of 2.0 [mm] (“CR/CR2.0”). The amount of wall thinning ($t_{n_{min}}$) in the case of using a full rivet and a rivet with a 1.0 [mm] hole (“CR/

CR1.0”) did not change. A significant increase in wall thickness was observed when the diameter of the hole in the rivet was increased to 2.0 [mm] (“CR/CR2.0”). For the rivet with the hole with a certain depth, instability of changes in the values of the t_u and ($t_{n_{min}}$) parameters was observed (Fig. 21). The values were lower than for the solid rivet and the rivet with a through hole. However, the value of wall thinning ($t_{n_{min}}$) in the case of a hole with a diameter of 2.0 [mm] (“CR/CR-2.0”) decreased by 3.7% (compared to the joint with a solid rivet). In combination with a hole rivet with depth 3.0 [mm] and diameter of 1.5 [mm], a higher value of ($t_{n_{min}}$) was obtained than for the rivet I (increase by 9.25%)—Fig. 21b.

The use of a rivet with a through hole with different diameter and a rivet with a hole depth of 3.0 [mm] resulted in changes in the geometrical parameters of the embossment (Fig. 22). Changing these parameters affects the formation of an interlock (Fig. 21). The analysis of the above results shows that the diameter of the hole in the rivet for which significant changes were obtained was 2.0 [mm] (Figs. 21, 22). The larger the diameter of the hole in the rivet, the greater was the change in the maximum diameter of the upper sheet in the joint interlock (d_2) (Fig. 22a). The largest reduction in diameter d_2 was obtained when the hole in the rivet was increased from 2 [mm] to 2.5 [mm]. However, the use of a rivet with a hole made at a certain depth caused smaller changes in the d_2 diameter. The effect of a through hole and a hole made at a certain depth had a similar effect on changes in the minimum distance between the upper and lower sheets (h_3). The smaller the hole in the rivet, the greater part of its material is upset, which causes a greater displacement of

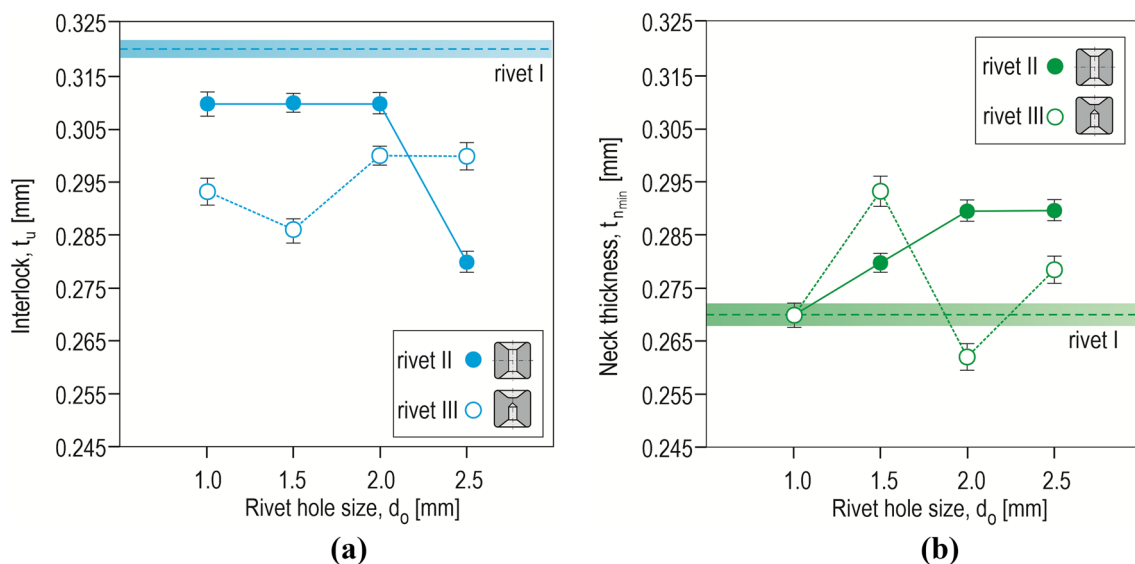


Fig. 21 The influence of the diameter of the rivet hole on the t_u —(a) and $t_{n_{min}}$ interlock parameters—(b). For rivet with through hole and rivet with a hole depth of 3.0 [mm]

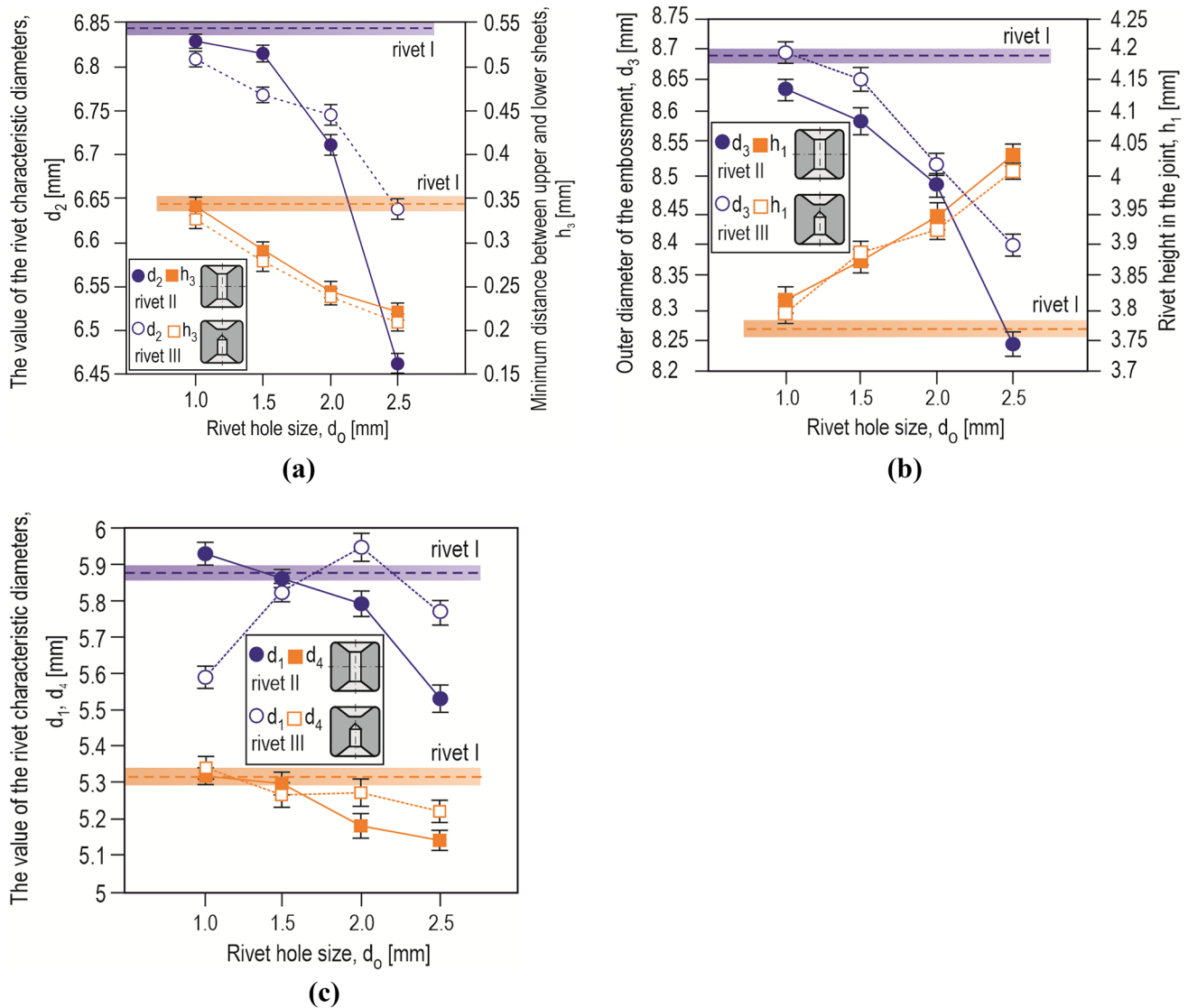


Fig. 22 The influence of the type and diameter of the rivet hole, used to form clinch-rivet joints, on the geometrical parameters of the interlock—(a–c)

the sheet material in the radial direction, thus increasing the maximum diameter of the embossment (d_3)—Fig. 22b.

Changes in the height of the rivet with the hole in the joint interlock were proportional to the values of the diameter of the through hole (Fig. 22b). In the case of a rivet with a hole made to a certain depth, the changes in the height of the rivet in the joint interlock were not linear. Differences in the outline of rivets with a through hole and those made to a certain depth are also visible in Fig. 18b. The use of a rivet with a hole reduced the maximum forming force and energy consumption (Fig. 16). A better effect was shown by using a rivet with a through hole than made to a certain depth.

During the formation of the “CR” connection, the rivet was upset, and its material flows in the radial direction, pushing the joined sheets out. In the lower part of the rivet,

its diameter (d_1) was the largest (Fig. 22c). In experimental tests of the joint forming process with different arrangements of the shape and geometry of the rivet, there was no loss of material cohesion (Figs. 16b, 18a). The highest radial flow of the rivet material was observed for the rivet with a 1.0 [mm] diameter through hole (Fig. 22c). And for a rivet with a hole at a certain depth, the highest radial flow was observed for a hole diameter of 2.0 [mm] ($d_o = 2.0$ [mm]).

The process of joining body elements can be carried out using an additional connector, without pressing it in as strongly as in the case of clinch-riveting process [35]. If the upper sheet is difficult to deform, it was proposed to make a hole and use a friction welded element (resistance element welding process “REW”).

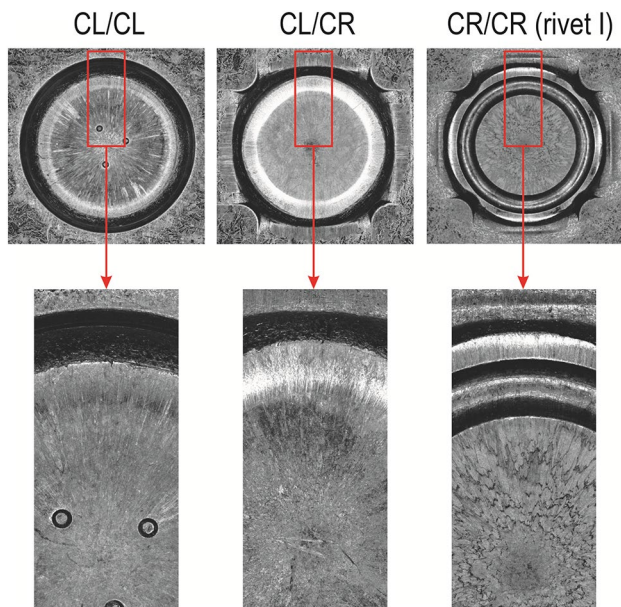


Fig. 23 The zoomed fragments of the outer surface of the embossment of the joint made with different tools

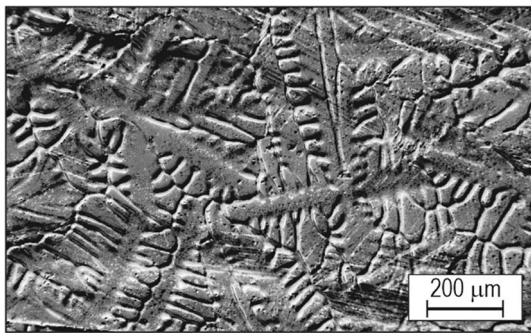


Fig. 24 The macrostructure of the sheet surface of the Zn coating before joint formation

3.3 Results of Degradation and Deviation of the Sheet Surface

The implementation of the “*Industry 5.0*” idea results in the automation of production processes and the introduction of intelligent quality control systems. Vision systems to observe the shape and geometry can be used to control the quality of the pressed joints. A robotic station with a manipulator and a vision system that inspects the “SPR” joint in a thin-walled structure was presented in a recently published work [81].

In the area of joint embossment, the bottom surface of the sheet was observed. Observation on the microscope allowed for the analysis of changes in the surface of the galvanised sheet. For individual characteristic areas of the embossment,

photographs were taken (Fig. 23). The state of the sheet surface with the zinc coating before joining is shown in Fig. 24. Areas with characteristic changes in the embossment surface were subjected to a more detailed analysis. The analysis made it possible to observe the effect of the arrangement of the joint forming tools on surface degradation (Fig. 25). In the case of forming the “CR/CR” joint, the pressure of the rivet on the lower plate blocked the radial movement of the sheet material. The Zn coating accumulated at the bottom of the die groove. Figure 26 shows the limit of accumulation of the zinc coating.

Measurement with an optical scanner allowed for 3D visualisation of the surface deformation of the material and observation of changes in the embossment, especially in areas of contact with the edges of the tools used (Fig. 27). For the appropriate cross-sectional planes, measurement paths were prepared for the value of sheet surface deviation from the initial position (as shown in Fig. 11).

The joining of sheets with an anticorrosion coating slightly changes the course of the forming force–displacement diagram and changes the condition and thickness of the Zn coating [82]. During the plastic forming of the material of the joined sheets, the external surface of the sheets is degraded. When sheets are joined using clinch-riveting technology, the rivet fills the joint space from the side of the punch system. The deformed material of the upper sheet is filled with a rivet at the place where an additional rivet is pressed. However, the material of the bottom sheet (outer side of the embossment) is only protected by a Zn coating. When a clinch-rivet joint is formed, the material of the bottom sheet is pressed into the die cavity. The Zn coating is deformed together with the material of the lower sheet (Fig. 25). As a result, the zinc coating is degraded in characteristic areas of the outer surface of the lower sheet. The greatest degradation of the surface of the bottom sheet during the forming tests occurred in the case of formation of the “CL/CL” joint (Fig. 25f). On the surface of the bulge of the embossment, macrogrooves are visible in a specific direction. In the case of the “CL/CR” joints, the bulge of the embossment is larger, however, such large discontinuities of the material did not occur (Fig. 25g). The fixed segments of the “SKB” die block circumferential deformation of the material. The use of a deformable rivet to form the clinch-rivet joints resulted in a reduction in material discontinuities (Fig. 25h). The rivet used was deformed during sheet metal pressing. In place of the smallest plastic flow of the bottom sheet material (in the vicinity of the joint axis), the surface pressures were the highest. Therefore, the possibility of plastic flow was the smallest (Fig. 25d). The use of an additional rivet instead of a rigid punch resulted in the fact that the material of the bottom sheet could be moved to a greater extent

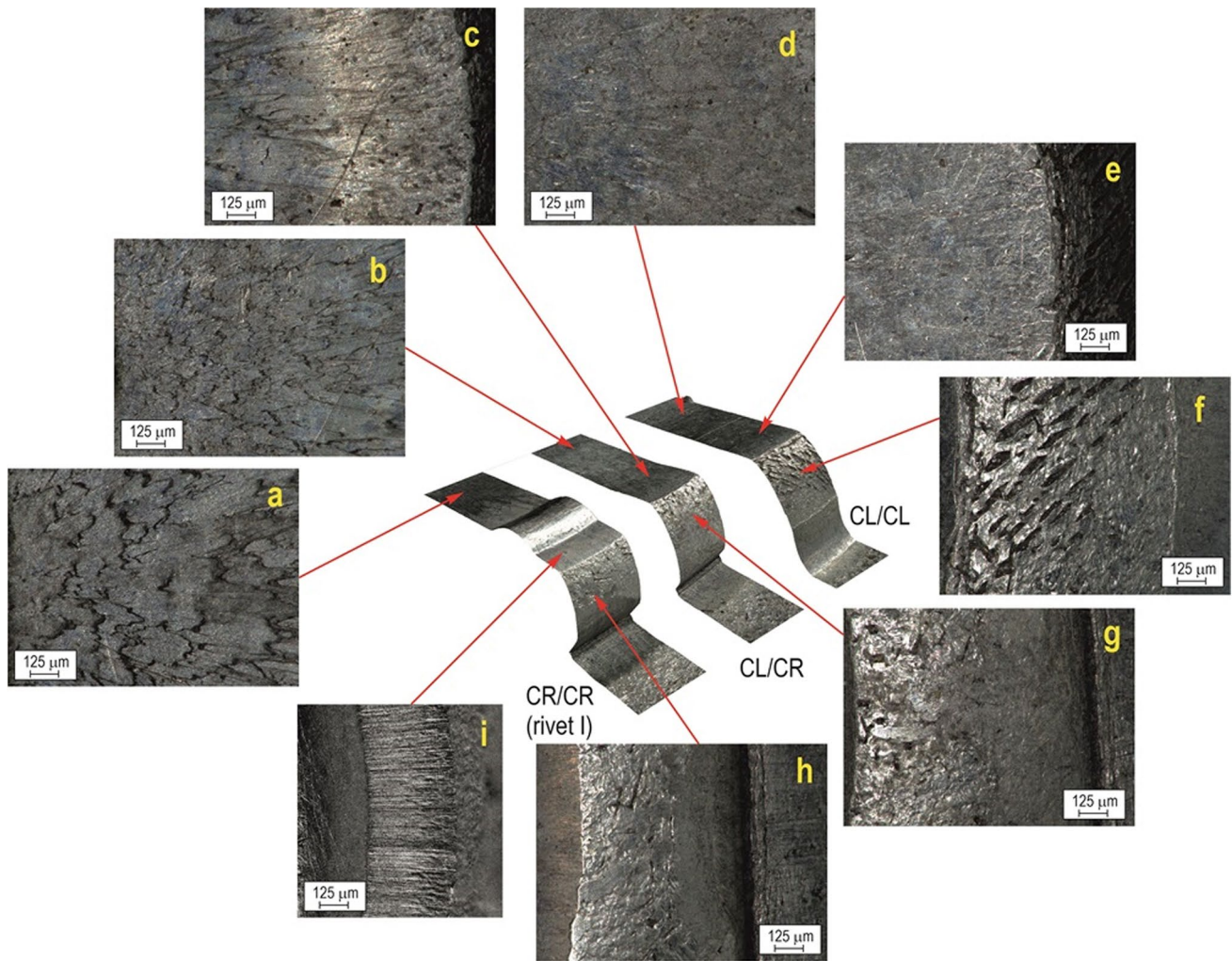


Fig. 25 The macrostructure of the sheet surface in the characteristic places of embossment

in the radial direction. Such a state of impact of the rivet and tools on the lower plate resulted in the formation of characteristic macroflow areas (Fig. 25a). Changing the “CL” rigid die to an “SKB” die with sliding segments resulted in greater flow of the material, i.e. with reduced resistance of the lower sheet (Fig. 25b). There, the bottom sheet material came into contact with the die, and plastic flow was accompanied by lower flow resistance. Hence, smaller steps of adhesive retention of the flowing material were formed on the surface.

The smallest degradation of the outer surface of the lower sheet occurred in the case of forming a joint with the punch (Fig. 25c). Both in the case of using the “CL/CR” and “CR/CR” tool systems, there was a directed material flow on the edge of the movable segments. The friction occurring between the movable segments and the lower sheet caused the formation of grooves (Fig. 25i). In the case of the “CL/CL” connection, the area close to the outer surface of the

embossment was above the die groove and was not limited by friction (Fig. 25e).

The clinch-rivet joint formation process has been well characterised in [52]. Figure 26 shows a characteristic fragment of the embossment of the joint with the use of the rivet I. In area 1, directional surface deformations of the sheet material with a zinc coating are visible (Fig. 26). The sheet material pressed into the free space of the die groove gradually fills it until the moment when its further filling requires pushing it out towards the outside of the die. A boundary (area 2) of the accumulated zinc coating material was formed in the circle located at the bottom of the die groove. In area 3, the sheet and the coating material were pushed outside the die groove. The plastically flowing material contact the outer edge of the die groove. The material moving in the radial direction was subjected to strong interaction, hence the directional cracks (area 4). The cracks in the lower sheet were created in the final phase of joint formation. In the last phase, there is a strong movement of

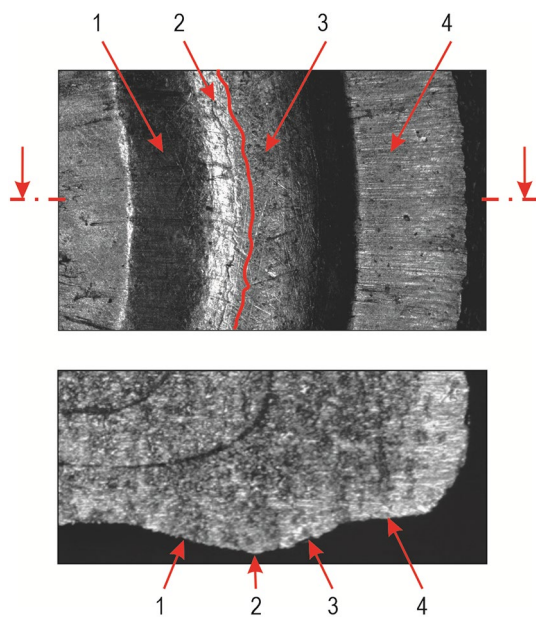


Fig. 26 The embossment area near the material outflow for the clinch-rivet joint (1—internal surface of the embossment, 2—edge of the embossment, 3—external surface of the embossment, 4—surface of the material flowing between the solid segments of the die)

the rivet material (in its lower part) and the sheets in the direction of the movement of the movable segments of the “SKB” die. The ZnNi coating at this place is subject to significant degradation. Degradation of the surface of sheets in the place of embossment reduces resistance to corrosion [83, 84]. The joining of steel sheets and aluminium alloy is a common case in thin-walled structures. In the case of joints with rivets II and III, the characteristic areas of embossment were very similar to the joint with rivet I (Figs. 23c, 27). For the joint with the largest diameter ($d_o = 2.5$ [mm]), a material bulge was formed with the smallest diameter d_3 was formed (Figs. 22b, 27).

In the case of forming the “CL/CL” joint, a large rounding (2) of the bottom sheet bend was formed, and the ring of the bulging material (1) does not have a clearly rounded shape (Fig. 28a). The use of the “SKB” die resulted in the formation of characteristic areas on the outer surface of the embossment resulting from the impact of the fixed (4) and movable (5) segments of the die (Fig. 28b). The ring was not formed in this case either (Fig. 23b). The material was slightly pressed out, but most of the material flowed plastically in a direction radial to the die axis. The use of an additional rivet caused that the material of the lower sheet completely filled the die groove (6)—Fig. 28c. In the last phase of the forming process, the rivet flows intensively in its lower part and pushes the sheet material in the radial direction.

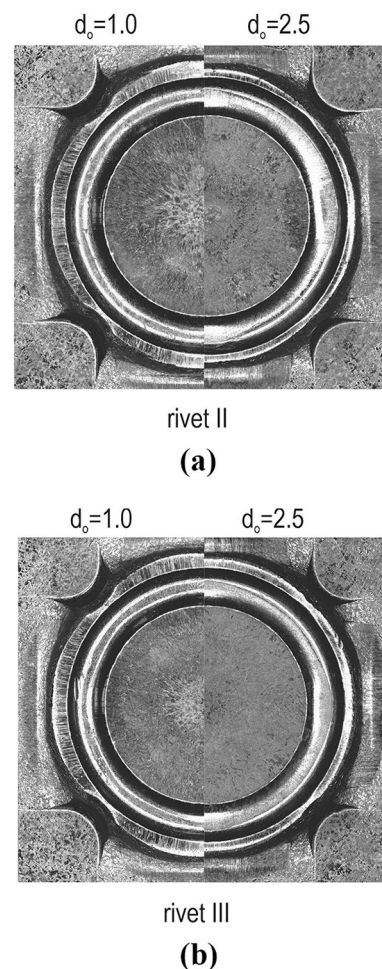


Fig. 27 The view of the embossment for rivets II and III with different hole diameter (d_o in [mm])

In each of the three types of tools arrangements, different maximum sheet deviations were observed. The deviations of the sheets are different from those shown in Fig. 2a. In all analysed cases, both sheets were bent in the same direction according to the diagram shown in Fig. 29. The outline of the upper and lower surfaces of the sheet for joints formed with different tools is shown in Fig. 30. The largest deviation of the sheets was measured on the “CL/CL” joint sample, the smallest for the variant of the tools used to form the “CL/CR” joint. In the case of using a rivet II, the highest strip deviation was observed for a hole in the rivet with a diameter of 1.5 [mm], both for the upper (Fig. 31a) and bottom (Fig. 31b) sheets. A similar situation occurred for joints formed with rivet III (Fig. 32). However, the difference in the deviation of the sheets between the connection with the rivet III ($d_o = 1.5$ [mm]) and the rivet I was smaller than in the case of the rivet II (Figs. 31, 32). The smallest deviation of the upper and lower sheets was observed for the joints with a rivet

Fig. 28 The view of the embossment after 3D measurement scan of the lower sheet: **a** “CL/CL” joint, **b** “CL/CR” joint, **c** “CR/CR” joint

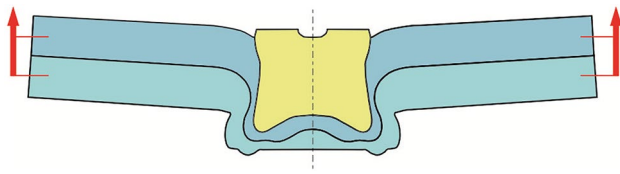
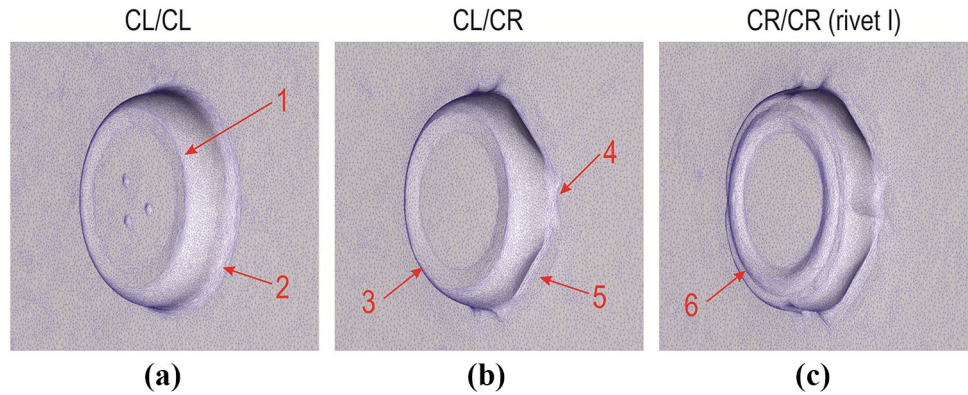


Fig. 29 The directions of the sheet deviations for sample with 40×40 [mm] dimensions

with a hole diameter of 2.5 [mm]. Figures 30, 31 and 32 also include the values of the circles measured on the base surface of the upper and lower plates at which the deviations of the plates were equal to zero. Depending on the joining technique used, deformations of different values are obtained in the sheets [5, 8]. From the point of view of the tightness of the connection, it is important that the sheets between them do not bend and that the corrosive agent does not penetrate the joint between the joined sheets. The conducted research [83, 84] showed that both

electrochemical and galvanic corrosion reduce the load capacity of the clinch joint.

3.4 Maximum Load Capacity and Energy Dissipation in the Strength Test of the Joints

Figure 33 shows the shear force–displacement diagrams obtained in the strength test for the lap joint. The area under the curve is the basis for determining the energy consumption of the joint failure according to the guidelines provided in the ISO 12996:2013 standard [73]. For joints formed with different tools arrangement, the joints were characterised by maximum load capacity for various values of displacement (s). Different values of the maximum forming force were obtained during the joint formation process (Fig. 34). The highest forming forces were obtained for the case of using the rivet and the “SKB” die. For this combination, the highest joint load capacity was also obtained in the shear test. The “SKB” die is characterised by four fixed and four movable segments. The profile of the die groove is close to

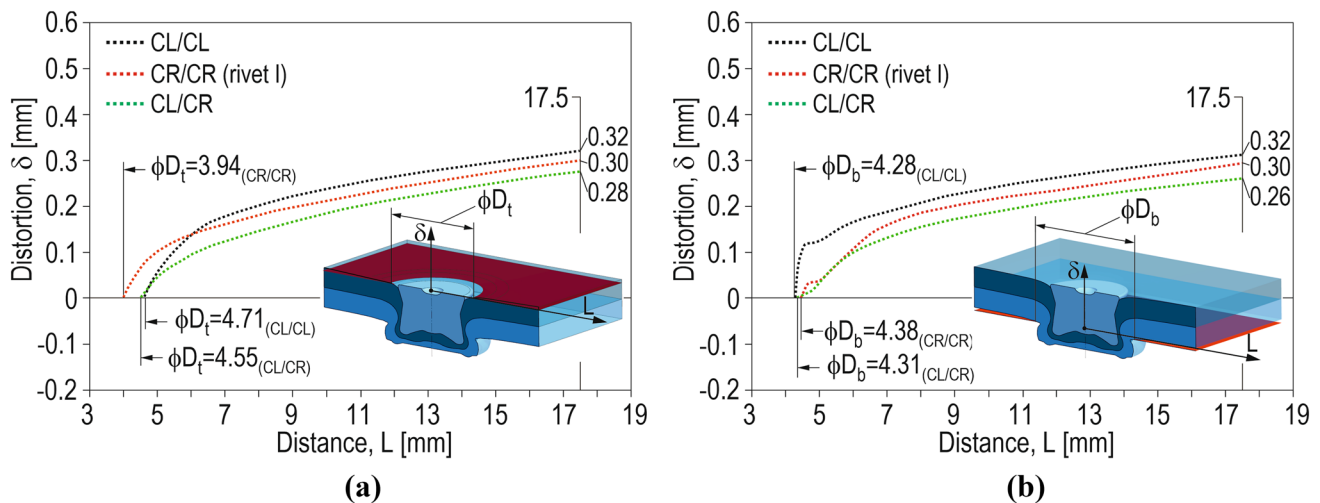


Fig. 30 The deviations of the sheet edge outline (in [mm]): **a** upper, **b** lower, for different arrangement of joining tools

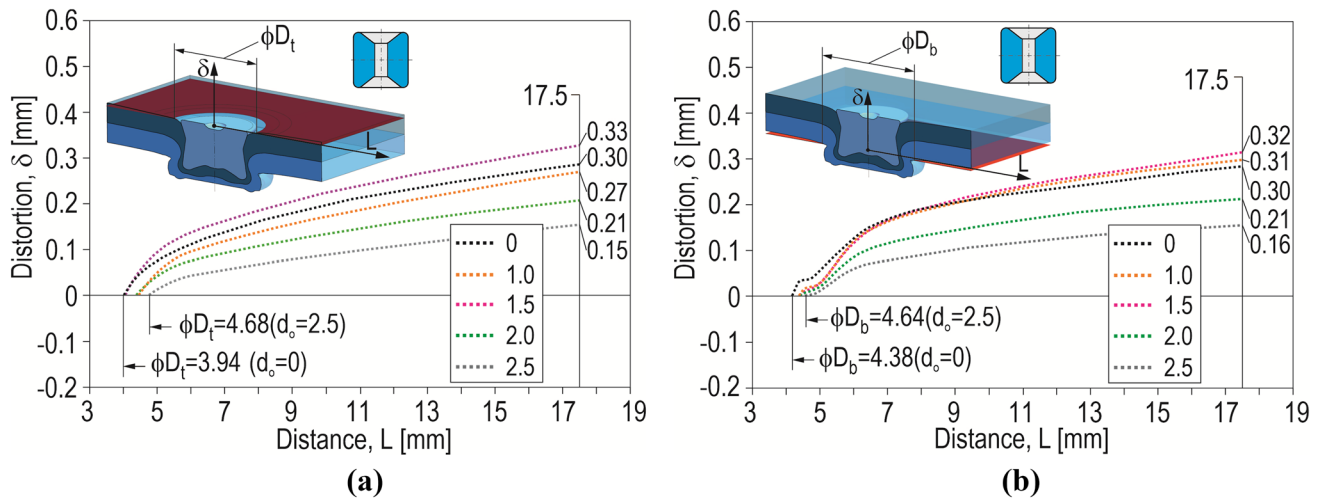


Fig. 31 The deviations of the sheet outline for the rivet with a through hole and different hole dimension (d_o in [mm]): **a** upper, **b** lower

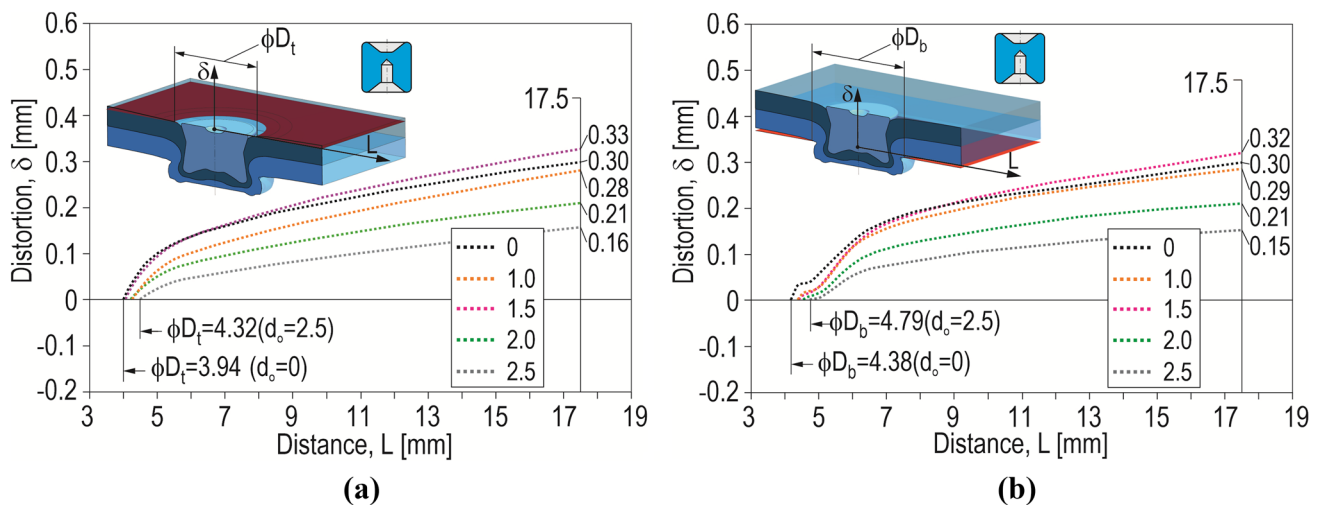


Fig. 32 The deviations of the sheet outline for the rivet with a certain depth hole and different hole dimension (d_o in [mm]): **a** upper, **b** lower

a rectangle. The formation of clinch joints is possible using tools with a round profile and movable segments without fixed segments. This die design allows for the joining of more material in different arrangements [85].

The parameter values for the clinch joint (“CL/CL”) were the reference point. Using a round die instead of a rigid die resulted in a 9% reduction in the forming force. The maximum load capacity was at a similar level. The use of a set of tools to form clinch-rivet joints with a rivet without a hole resulted in an increase in the forming force of 24%. However, the maximum joint load capacity increased by 88%.

The shear force–displacement diagrams were very similar for the joint with and additional rivet. Examples of the shear test diagrams for joints with the smallest and largest rivet holes are shown in Fig. 35. The maximum joint shear force

was obtained for rivet I (Fig. 36). The highest energy consumption of joint failure was obtained in the case of connection with a rivet III ($d_o = 1.5$ [mm]). Compared to solid rivet, the use of a 2.5 [mm] hole (rivet II) significantly reduced the required joint forming force by 22.5% (Fig. 16), and the maximum load capacity decreased by 3.8% (Fig. 36). The forming force of the joint with the rivet II was 2.8% lower compared to that of the “CL/CL” joint (Figs. 34, 36), and the maximum shear force was 81.5% higher. Therefore, it was reasonable to modify the full rivet to the version with a hole. For the rivet III, apart from the case with a 1.5 [mm] hole, slightly higher load values were obtained than for the joint with the rivet II.

The shear force–displacement diagrams were very similar for the joint with and additional rivet. Examples of the shear

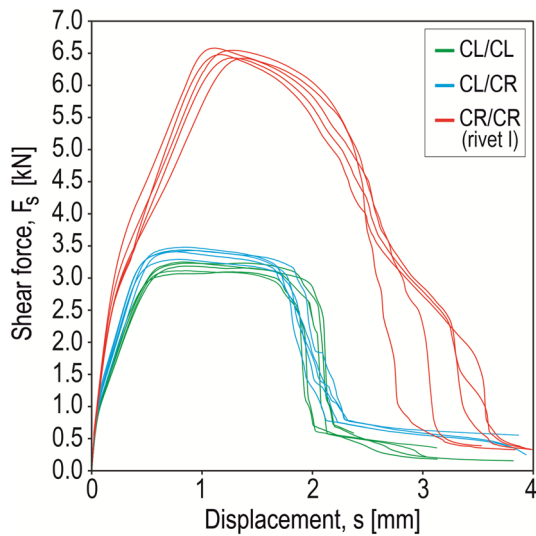


Fig. 33 The shear force–displacement diagrams for joint formed by using different tools

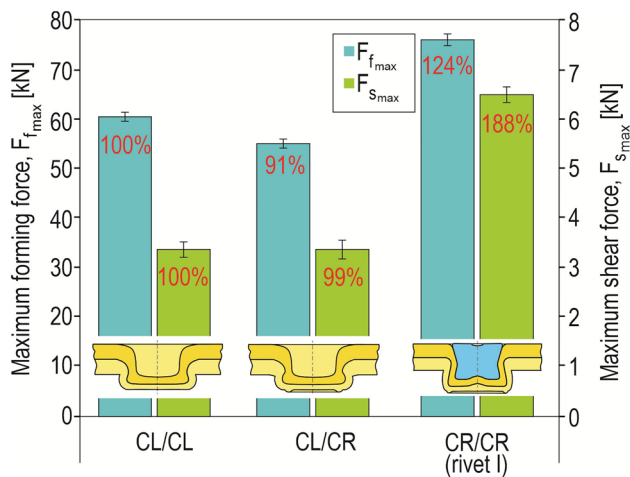


Fig. 34 The comparison of the forming force and the maximum shear force for joints formed with different tool arrangements

test diagrams for joints with the smallest and largest rivet holes are shown in Fig. 35. The maximum joint shear force was obtained for rivet I (Fig. 36). The highest energy consumption of joint failure was obtained in the case of connection with a rivet III ($d_o = 1.5$ [mm]). Compared to solid rivet, the use of a 2.5 [mm] hole (rivet II) significantly reduced the required joint forming force by 22.5% (Fig. 16), and the maximum load capacity decreased by 3.8% (Fig. 36). The forming force of the joint with the rivet II was 2.8% lower compared to that of the “CL/CL” joint (Figs. 34, 36), and the maximum shear force was 81.5% higher. Therefore, it was reasonable to modify the full rivet to the version with a hole. For the rivet III, apart from the case with a 1.5 [mm]

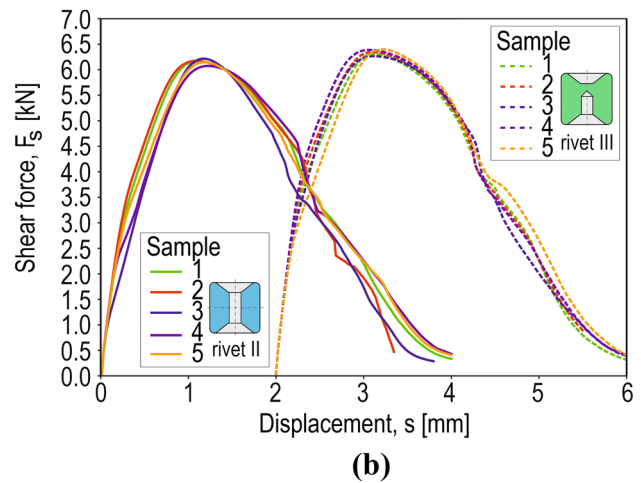
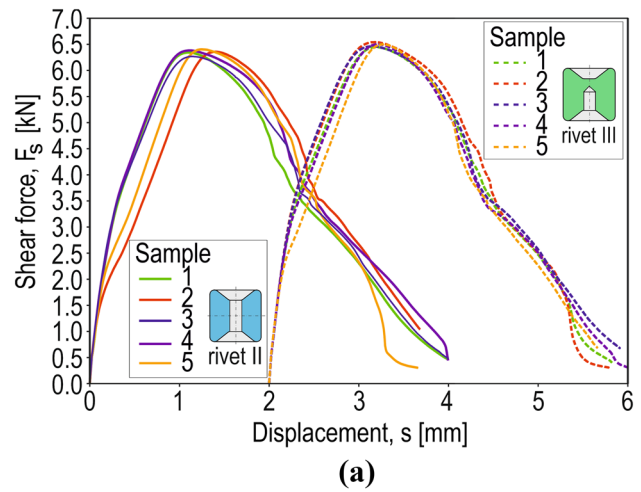


Fig. 35 The shear force–displacement diagram of a lap joint with a rivet with through hole and hole with a certain depth— d_o : **a** 1.0 [mm], **b** 2.5 [mm]

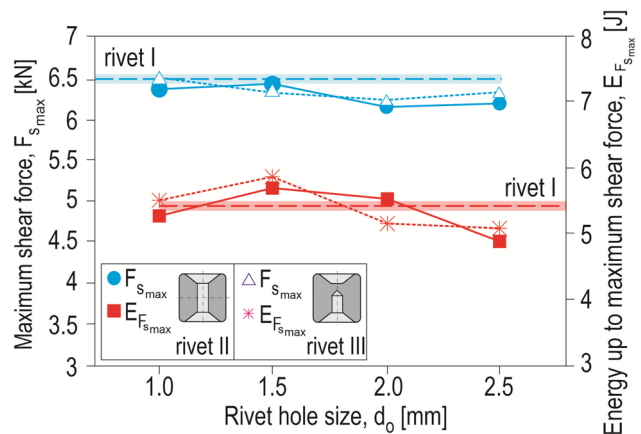


Fig. 36 The average values of maximum shear force and energy up to maximum shear force for different rivet geometry

hole, slightly higher load values were obtained than for the joint with the rivet II.

4 Summary and Conclusions

The presented paper explains the influence of the use of different construction of tools and an additional steel rivet with a hardness of 400HV1 and rivet modification on the energy consumption of the joint and on the macrostructure of the joint. Using the results presented for joints forming examples, new observations were formulated on the behaviour of the material, changes on the embossment surface depending on the forming method, and in particular the energy consumption of the joining processes. It is possible to significantly strengthen the clinch joint by an additional deformable element in the form of a steel rivet without disturbing the cohesion of the sheet material. This paper concerned several aspects related to the formation of an interlock in a clinch-rivet joint, changes in the geometry of the joint, deformation of sheets as a result of local impact with tools, and an additional rivet. The most important and significant information obtained from the conducted research is as follows:

1. The use of the "SKB" die with movable and fixed elements allowed for reducing the forming force by 9% and the joint forming energy consumption by 5% compared to the case of using a solid round die. The use of an additional solid rivet to form the joint resulted in an increase in forming force by 124% and forming energy consumption by 66% compared to the case of using solid round "CL/CL" tools (without a rivet).
2. The use of a rivet with a hole up to $=2.5$ [mm] allowed for a reduction of the maximum forming force compared to the case of forming with a solid rivet by 22.5% (for rivet II) and by 10.5% (for rivet III). The use of rivets II (with a through hole) allowed to reduce the energy consumption of the joining process by 15.5%, and for rivet III by 11%, compared to the case of using a solid rivet.
3. Among the three arrangements of the joint forming process, the highest interlock value (t_u) was obtained for the case of using a die with movable segments and a solid rivet. The size t_u of the interlock was 180% larger than in the case of a joint made with a solid round die ("CL/CL"). In combination with a rivet II (for hole depth $do=2.5$ [mm]), the t_u value was reduced by 12.5% compared to the joint with a solid rivet.
4. The deviation of the sheet metal surface in the case of a joint formed using a special "SKB" die with movable segments ("CL/CR") was smaller than in the case of a simpler solid round die ("CL/CL"). The maximum deviation on the measured sheets decreased by 12.5% (for the upper sheet) and by 18.75% (for the lower sheet). The use of an additional full rivet (rivet I), to increase the load capacity of the joint, formed using the "SKB" die resulted in an increase in the deviation of the sheets compared to the joint formed without a rivet ("CL/CR") by 6.7% (for the upper sheet) and by 13.4% (for the lower sheet).
5. The deviations of the lower and upper sheets for all analysed cases of forming tool arrangement were in the same direction, and the deviation values at the highest distance tested from the joint axis had similar values. The use of a rivet II with a hole instead of a full rivet (rivet I) resulted in a reduction in the deviation of the upper sheets by 50% and for the lower sheet by 46.7%. Very similar values were obtained when using rivet III (with a hole of 2.5 [mm]) and a similar reduction in the deflection of the sheets was achieved.

Author contributions JM: Writing—review & editing, Writing—original draft, Visualization, Validation, Supervision, Project administration, Methodology, Investigation, Formal analysis, Conceptualization. ŁB: Writing—original draft, Visualization, Validation, Software, Methodology, Investigation, Data curation, Conceptualization. WW: Writing—original draft, Visualization, Validation, Software, Methodology, Investigation, Data curation, Conceptualization.

Data availability The data presented in this study are available on request from the corresponding author due to privacy.

Declarations

Conflict of interest All authors have contributed to, read, and approved the manuscript in its current form and there are no conflicts of interest to declare. We declare that none of the work contained in this manuscript has been published in any language, nor is it currently under consideration by any other journal.

Open Access This article is licensed under a Creative Commons Attribution 4.0 International License, which permits use, sharing, adaptation, distribution and reproduction in any medium or format, as long as you give appropriate credit to the original author(s) and the source, provide a link to the Creative Commons licence, and indicate if changes were made. The images or other third party material in this article are included in the article's Creative Commons licence, unless indicated otherwise in a credit line to the material. If material is not included in the article's Creative Commons licence and your intended use is not permitted by statutory regulation or exceeds the permitted use, you will need to obtain permission directly from the copyright holder. To view a copy of this licence, visit <http://creativecommons.org/licenses/by/4.0/>.

References

- Heeren, R., & Timmermann, R. (2002). *Mechanical joining in the automotive industry*. SMWC X, Paper No. 4-1.
- Zhou, Y., Lan, F., & Chen, J. (2010). Influence of tooling geometric parameters on clinching joint properties for steel-aluminum car-body structures. In *Proceedings of 3rd IEEE International Conference on Computer Science and Information Technology; ICCSIT* (pp. 441–445). <https://doi.org/10.1109/ICCSIT.2010.5564063>.
- Mucha, J. (2017). Clinching technology in the automotive industry. *The Archives of Automotive Engineering – Archiwum Motoryzacji*, 76, 75–94. <https://ee.tox-pressotechnik.com> (23.05.2023).
- Meschut, G., Janzen, V., & Olfemann, T. (2014). Innovative and highly productive joining technologies for multi-material lightweight car body structures. *Journal of Materials Engineering and Performance*, 23, 1515–1523. <https://doi.org/10.1007/s11665-014-0962-3>.
- <https://global.abb> (23.05.2023).
- Heyser, P., Wiesenmayer, S., Frey, P., et al. (2022). Consideration of the manufacturing history of sheet metal components for the adaptation of a clinching process. *Proceedings of The Institution of Mechanical Engineers Part L-Journal of Materials-Design and Applic*, 236, 1203–1215. <https://doi.org/10.1177/14644207221077>
- Eckert, A., Neugebauer, R., Rössinger, M., et al. (2011). Application limits of a method to predict distortion caused by mechanical joining technologies in Car body construction. In *The 8th international conference and workshop on numerical simulation of 3D sheet metal forming processes (NUMISHEET 2011)*, Seoul, Republic of Korea, 21–26 August, pp. 251–258. <https://doi.org/10.1063/1.3623618>.
- Hahn, O., Meschut, G., Suellentrop, S., Janzen V., & Olfemann, T. (2013). *Joining technologies in hybrid lightweight structures* (in German), Leichtbau der Fahrzeugtechnik, H. Friedrich, Springer Vieweg Verlag, Wiesbaden, Germany, pp. 622–662. <https://doi.org/10.1007/978-3-658-12295-9>.
- Long, J., Lan, F., Chen, J., et al. (2009). Experimental investigation of the joints of mechanical clinching in the steel aluminum hybrid structure car body. *Journal of Plasticity Engineering*, 16, 88–94. <https://doi.org/10.1016/j.jmapro.2017.01.015>
- Bartczak, B., Mucha, J., & Trzepieciński, T. (2013). Stress distribution in adhesively bonded joints and the loading capacity of hybrid joints of car body steels for the automotive industry. *International Journal of Adhesion and Adhesives*, 45, 42–52. <https://doi.org/10.1016/j.ijadhadh.2013.03.012>
- Saberi, S., Enzinger, N., Vallant, R., et al. (2008). Influence of plastic anisotropy on the mechanical behavior of clinched joint of different coated thin steel sheets. *International Journal of Material Forming*, 1, 273–276. <https://doi.org/10.1007/s12289-008-0349-9>
- Mucha, J., Kaščák, L., & Spišák, E. (2011). Joining the car-body sheets using clinching process with various thickness and mechanical property arrangements. *Archives of Civil and Mechanical Engineering*, 1, 135–148. [https://doi.org/10.1016/S1644-9665\(12\)60179-4](https://doi.org/10.1016/S1644-9665(12)60179-4)
- Zhang, X., Chen, C., & Peng, H. (2022). Recent development of clinching tools and machines. *International Journal of Advanced Manufacturing Technology*, 121, 2867–2899. <https://doi.org/10.1007/s00170-022-09428-1>
- Zhang, Y., Wang, C., Shan, H., Li, Y., & Luo, Z. (2018). High-toughness joining of aluminum alloy 5754 and DQSK steel using hybrid clinching–welding process. *Journal of Materials Processing Technology*, 259, 33–44. <https://doi.org/10.1016/j.jmatprotec.2018.04.021>
- Džupon, M., Kaščák, L., Čmorej, D., Čiripová, L., Mucha, J., & Spišák, E. (2023). Clinching of high-strength steel sheets with local preheating. *Applied Sciences*, 13, 7790. <https://doi.org/10.3390/app13137790>
- Lee, C.-J., Shen, G., Kim, B.-M., Lambiase, F., & Ko, D.-C. (2018). Analysis of failure-mode dependent joint strength in hole clinching from the aspects of geometrical interlocking parameters. *Metals*, 8, 1020. <https://doi.org/10.3390/met8121020>
- He, X., Pearson, I., & Young, K. (2008). Self-pierce riveting for sheet materials: State of the art. *Journal of Materials Processing Technology*, 199, 27–36. <https://doi.org/10.1016/j.jmatprotec.2007.10.071>
- Ang, H. Q. (2021). An overview of self-piercing riveting process with focus on joint failures, corrosion issues and optimisation techniques. *Chinese Journal of Mechanical Engineering*, 34, 1–25. <https://doi.org/10.1186/s10033-020-00526-3>
- Xing, B., He, X., Zeng, K., et al. (2014). Mechanical properties of self-piercing riveted joints in aluminum alloy 5052. *International Journal of Advanced Manufacturing Technology*, 75, 351–361. <https://doi.org/10.1007/s00170-014-6152-5>
- Zhang, X., He, X., Gu, F., & Ball, A. (2019). Self-piercing riveting of aluminium–lithium alloy sheet materials. *Journal of Materials Processing Technology*, 268, 192–200. <https://doi.org/10.1016/j.jmatprotec.2019.01.019>
- Zhao, L., He, X., Xing, B., Zhang, X., Cheng, Q., Gu, F., & Ball, A. (2017). Fretting behavior of self-piercing riveted joints in titanium sheet materials. *Journal of Materials Processing Technology*, 249, 246–254. <https://doi.org/10.1016/j.jmatprotec.2017.06.016>
- He, X., Wang, Y., Lu, Y., et al. (2015). Self-piercing riveting of similar and dissimilar titanium sheet materials. *International Journal of Advanced Manufacturing Technology*, 80, 2105–2115. <https://doi.org/10.1007/s00170-015-7174-3>
- Neugebauer, R., Jesche, F., & Israel, M. (2010). Enlargement of the application range of solid punch riveting by two-piece dies. *International Journal of Material Forming*, 3, 999–1002. <https://doi.org/10.1007/s12289-010-0938-2>
- Mucha, J. (2013). The effect of material properties and joining process parameters on behavior of self-pierce riveting joints made with the solid rivet. *Materials & Design*, 52, 932–946. <https://doi.org/10.1016/j.matdes.2013.06.037>
- Mucha, J. (2014). The numerical analysis of the effect of the joining process parameters on self-piercing riveting using the solid rivet. *Archives of Civil and Mechanical Engineering*, 14, 444–454. <https://doi.org/10.1016/j.acme.2013.11.002>
- Mucha, J. (2015). The failure mechanics analysis of the solid self-piercing riveting joints. *Engineering Failure Analysis*, 47, 77–88. <https://doi.org/10.1016/j.engfailanal.2014.10.008>
- Han, D., Yang, K., & Meschut, G. (2011). Mechanical joining of glass fibre reinforced polymer (GFRP) through an innovative solid self-piercing rivet. *Journal of Materials Processing Technology*, 296, 117–182. <https://doi.org/10.1016/j.jmatprotec.2021.11.7182>
- Vorderbrüggen, J., Köhler, D., Grüber, B., Troschitz, J., Gude, M., & Meschut, G. (2022). Development of a rivet geometry for solid self-piercing riveting of thermally loaded CFRP-metal joints

- in automotive construction. *Composite Structures*, 291, 115583. <https://doi.org/10.1016/j.compstruct.2022.115583>
30. Colligan, K. J., Konkol, P. J., Fisher, J. J., & Pickens, J. R. (2023). Friction stir welding demonstrated for combat vehicle construction. *Welding Journal*, 82, 34–40.
 31. Shen, Z., Ding, Y., Chen, J., Shalch Amirkhiz, B., Wen, J. Z., Fu, L., & Gerlich, A. P. (2019). Interfacial bonding mechanism in Al/coated steel dissimilar refill friction stir spot welds. *Journal of Materials Science & Technology*, 35, 1027–1038. <https://doi.org/10.1016/j.jmst.2019.01.001>
 32. Shen, Z., Ding, Y., Chen, J., & Gerlich, A. P. (2020). Advances in friction stir spot welding. *Critical Reviews in Solid State and Materials Sciences*, 45, 457–534. <https://doi.org/10.1080/10408436.2019.1671799>
 33. Groche, P., Wohletz, S., Brenneis, M., Pabst, C., & Resch, F. (2014). Joining by forming—A review on joint mechanisms, applications and future trends. *Journal of Materials Processing Technology*, 214, 1062–1093. <https://doi.org/10.1016/j.jmatprotec.2013.12.022>
 34. Draht, T. (2008). Joining in the automotive industry—One-sided joining without pre-hole (in German). *Lightweight Design*, 1, 20–23.
 35. Meschut, G., Hahn, O., Olfemann, T., & Janzen, V. (2014). Innovative joining technologies for multi-material structures. *Welding World*, 58, 65–75. <https://doi.org/10.1007/s40194-013-0098-3>
 36. He, X. (2017). Clinching for sheet materials. *Science and Technology of Advanced Materials*, 18, 381–405. <https://doi.org/10.1080/14686996.2017.1320930>
 37. Abe, Y., Kato, T., Mori, K., & Nishino, S. (2014). Mechanical clinching of ultra-high strength steel sheets and strength of joints. *Journal of Materials Processing Technology*, 10, 2112–2118. <https://doi.org/10.1016/j.jmatprotec.2014.03.003>
 38. Mucha, J., & Witkowski, W. (2014). The clinching joints strength analysis in the aspects of changes in the forming technology and load conditions. *Thin-Walled Structures*, 82, 55–66. <https://doi.org/10.1007/s43452-023-00653-3>
 39. Krztoń, H., Mucha, J., & Witkowski, W. (2016). The application of laboratory X-Ray micro-diffraction to study the effects of clinching process in steel sheets. *Acta Physica Polonica A*, 130, 985–987. <https://doi.org/10.12693/APhysPolA.130.985>
 40. Ge, Y., & Xia, Y. (2020). Mechanical characterization of a steel-aluminum clinched joint under impact loading. *Thin-Walled Structures*, 151, 106759. <https://doi.org/10.1016/j.tws.2020.106759>
 41. Kupfer, R., Köhler, D., Römisch, D., Wituschek, S., Ewenz, L., Kalich, J., Weiß, D., Sadeghian, B., Busch, M., Krüger, J., Neuser, M., Grydin, O., Böhnke, M., Bielak, C.-R., & Troschitz, J. (2022). Clinching of aluminum materials—Methods for the continuous characterization of process, Microstructure and properties. *Journal of Advanced Joining Processes*, 5, 100108. <https://doi.org/10.1016/j.jajp.2022.100108>
 42. Mucha, J. (2011). The analysis of rectangular clinching joint in the shearing test. *Eksplotacja i Niezawodność – Maintenance and Reliability*, 3, 45–50.
 43. Zhang, Y., He, X., Wang, Y., et al. (2018). Study on failure mechanism of mechanical clinching in aluminium sheet materials. *International Journal of Advanced Manufacturing Technology*, 96, 3057–3068. <https://doi.org/10.1007/s00170-018-1734-2>
 44. Zhang, Y., He, X., Zeng, K., et al. (2017). Influence of heat treatment on mechanical properties of clinched joints in titanium alloy sheets. *International Journal of Advanced Manufacturing Technology*, 91, 3349–3361. <https://doi.org/10.1007/s00170-017-0019-5>
 45. Lambiasi, F., & Di Ilio, A. (2018). Joining aluminum with titanium alloy sheets by mechanical clinching. *Journal of Manufacturing Processes*, 35, 457–465. <https://doi.org/10.1016/j.jmapro.2018.09.001>
 46. He, X., Zhang, Y., Xing, B., Gu, F., & Ball, A. (2015). Mechanical properties of extensible die clinched joints in titanium sheet materials. *Materials & Design*, 71, 26–35. <https://doi.org/10.1016/j.matdes.2015.01.005>
 47. He, X., Lei, L., Zhang, Y., & Xing, B. Y. (2017). Mechanical Properties and Fracture Analysis of Clinched Joints in Titanium Sheet Materials. *Acta Physica Polonica A*, 131, 16–19. <https://doi.org/10.12693/APhysPolA.131.16>
 48. Ren, X., & Chen, C. (2023). Research on mechanical clinching process for dissimilar aluminum alloy sheets with inclined surface. *Journal of Manufacturing Processes*, 89, 362–370. <https://doi.org/10.1016/j.jmapro.2023.01.073>
 49. Peng, H., Chen, C., Zhang, H., et al. (2020). Recent development of improved clinching process. *International Journal of Advanced Manufacturing Technology*, 110, 3169–3199. <https://doi.org/10.1007/s00170-020-05978-4>
 50. Kaščák, L., Spišák, E., & Mucha, J. (2012). Evaluation of properties of joints made by clinching and self-piercing riveting methods. *Acta Metallurgica Slovaca*, 18, 172–180.
 51. Mucha, J., Kaščák, L., & Spišák, E. (2013). The Experimental Analysis of forming and strength of clinch riveting sheet metal joint made of different materials. *Advances in Mechanical Engineering*. <https://doi.org/10.1155/2013/848973>
 52. Kaščák, L., Spišák, E., & Mucha, J. (2013). Clinchrivet as an alternative method to resistance spot welding. *Acta Mechanica et Automatica*, 7, 79–82. <https://doi.org/10.2478/ama-2013-0014>
 53. Mucha, J., Kaščák, L., & Witkowski, W. (2021). Research on the influence of the AW 5754 aluminum alloy state condition and sheet arrangements with AW 6082 aluminum alloy on the forming process and strength of the ClinchRivet joints. *Materials*, 14, 2980. <https://doi.org/10.3390/ma14112980>
 54. Mucha, J., Boda, L., & Witkowski, W. (2023). Geometrical parameters and strength of clinching joint formed with the use of an additional rivet. *Archives of Civil and Mechanical Engineering*, 114, 1–16. <https://doi.org/10.1007/s43452-023-00653-3>
 55. Mucha, J., Boda, L., Witkowski, W., & Poręba, M. (2023). Mixed-mode loading tests for determining the mechanical properties of clinched joints with an additional rivet used in the assembly of thin-walled structures. *Thin-Walled Structures*, 190, 110965. <https://doi.org/10.1016/j.tws.2023.110965>
 56. Chen, C., Zhang, X., Wen, C., & Yin, Y. (2022). Effect of blank holder force on joining quality of the flat clinch-rivet process. *International Journal of Advanced Manufacturing Technology*, 121, 6315–6323. <https://doi.org/10.1007/s00170-022-09744-6>
 57. Ren, X., Chen, C., Ran, X., Li, Y., & Zhang, X. (2021). Microstructure evolution of AA5052 joint failure process and mechanical performance after reconditioning with tubular rivet. *Transactions of Nonferrous Metals Society of China*, 31, 3380–3393. [https://doi.org/10.1016/S1003-6326\(21\)65736-9](https://doi.org/10.1016/S1003-6326(21)65736-9)
 58. Chen, C., Li, Y., Zhang, H., Li, Y., Pan, Q., & Han, X. (2020). Investigation of a renovating process for failure clinched joint to join thin-walled structures. *Thin-Walled Structures*, 151, 106686. <https://doi.org/10.1016/j.tws.2020.106686>
 59. Chen, C., Ran, X., Pan, Q., Zhang, H., Yi, R., & Han, X. (2020). Research on the mechanical properties of repaired clinched joints with different forces. *Thin-Walled Structures*, 152, 106752. <https://doi.org/10.1016/j.tws.2020.106752>
 60. Ren, X., Chen, C., Ran, X., Gao, X., & Gao, Y. (2021). Investigation on lightweight performance of tubular rivet-reinforced joints

- for joining AA5052 sheets. *Journal of the Brazilian Society of Mechanical Sciences and Engineering*, 43, 333. <https://doi.org/10.1007/s40430-021-03053-x>
61. Chen, C., Wu, J., & Li, H. (2021). Optimization design of cylindrical rivet in flat bottom riveting. *Thin-Walled Structures*, 168, 108292. <https://doi.org/10.1016/j.tws.2021.108292>
 62. Cai, W., Lesperance, R. M., Marin, S. P., Meyer, W. W., & Oetjens, T. J. (2002). Digital panel assembly for automotive body-in-white. ASME IMECE 2002-MED-32341.
 63. Cai, W., Wang, P. C., & Yang, W. (2005). Assembly dimensional prediction for self-piercing riveted aluminum panels. *International Journal of Machine Tools and Manufacture*, 45, 695–704. <https://doi.org/10.1016/j.ijmactools.2004.09.023>
 64. Tozaki, Y., Uematsu, Y., & Tokaji, K. (2007). Effect of tool geometry on microstructure and static strength in friction stir spot welded aluminium alloys. *International Journal of Machine Tools and Manufacture*, 47, 2230–2236. <https://doi.org/10.1016/j.ijmactools.2007.07.005>
 65. Hwang, Y.-M., Kang, Z.-W., Chiou, Y.-C., & Hsu, H.-H. (2008). Experimental study on temperature distributions within the work-piece during friction stir welding of aluminum alloys. *International Journal of Machine Tools and Manufacture*, 48, 778–787. <https://doi.org/10.1016/j.ijmactools.2007.12.003>
 66. Wrobel, N., Rejek, M., Królczyk, G., & Hloch, S. (2017). Testing of tight crimped joint made on a prototype Stand. *Lecture Notes in Mechanical Engineering*. https://doi.org/10.1007/978-3-319-68619-6_48
 67. Rejek, M., Wróbel, N., Królczyk, J., & Królczyk, G. (2019). Designing and testing cold-formed rounded connections made on a prototype station. *Materials*, 12, 1061. <https://doi.org/10.3390/ma12071061>
 68. Shan, H., Yang, B., Ma, Y., Lou, M., Feng, Q., Li, Y., & Lin, Z. (2022). Friction stud riveting (FSR) of thick high-strength aluminum alloy structure. *International Journal of Machine Tools and Manufacture*, 177, 103889. <https://doi.org/10.1016/j.ijmactools.2022.103889>
 69. EN 10346:2015. *Continuously hot-dip coated steel flat products for cold forming—Technical delivery conditions*. European Committee for Standardization, (2015).
 70. PN-EN ISO 6892-1:2020-05. (2020). *Metals - Tensile test—part 1: Room temperature test method*.
 71. ISO 6507-1:2018. (2018). *Metallic materials—Vickers hardness test—Part 1: Test method*. Technical Committee ISO/TC 164, Mechanical testing of metals, Subcommittee SC 3, Hardness testing.
 72. ASTM E-1508-12:2013. (2013). *Standard guide for quantitative analysis by energy-dispersive spectroscopy*. Committee E04 on Metallography. Subcommittee E04.11 on X-Ray and Electron Metallography.
 73. ISO 12996:2013. (2013). *Mechanical joining—Destructive testing of joints—Specimen dimensions and test procedure for tensile shear testing of single joints*. Technical Committee ISO/TC 44/SC 6 Resistance welding and allied mechanical joining.
 74. Markowski, T., Mucha, J., & Witkowski, W. (2013). FEM Analysis of clinching joint machine's C-Frame rigidity. *Eksplotacja i Niezawodność-Maintenance and Reliability*, 15, 51–57.
 75. Zhang, Y., Xu, H., Peng, R., et al. (2022). The state of the art of finite element analysis in mechanical clinching. *International Journal of Precision Engineering and Manufacturing-Green Technology*, 9, 1191–1214. <https://doi.org/10.1007/s40684-021-00366-z>
 76. Mucha, J. (2011). The analysis of lock forming mechanism in the clinching joint. *Materials & Design*, 32, 4943–4954. <https://doi.org/10.1016/j.matdes.2011.05.045>
 77. Hou, Y., Ding, K., Lu, G., et al. (2022). Investigation of micro-scale laser shock flat hole clinching. *International Journal of Precision Engineering and Manufacturing-Green Technology*, 23, 1019–1025. <https://doi.org/10.1007/s12541-022-00665-8>
 78. Kato, T., Abe, Y., & Mori, K. (2010). Plastic joining of aluminium alloy sheets by aluminium alloy cylinder. *Steel Research International*, 9, 1136–1139.
 79. Haque, R. (2018). Quality of self-piercing riveting (SPR) joints from cross-sectional perspective: A review. *Archives of Civil and Mechanical Engineering*, 1, 83–93. <https://doi.org/10.1016/j.acme.2017.06.003>
 80. Busse, S., Merklein, M., Roll, K., Ruther, M., & Zürn, M. (2010). Development of a mechanical joining process for automotive body-in-white production. *International Journal of Material Forming*, 1, 1059–1062. <https://doi.org/10.1007/s12289-010-0953-3>
 81. Lee, H., Kim, J., Guo, X., et al. (2023). Non-destructive inspection system for self-piercing riveting in CFRP-metal joining product using stereoscopic method with robotic manipulator. *International Journal of Precision Engineering and Manufacturing*, 24, 1625–1631. <https://doi.org/10.1007/s12541-023-00888-3>
 82. Abe, Y., Kato, T., Kishimoto, M., & Mori, K. (2010). Joining of hot-dip coated high-strength steel sheets by mechanical clinching. *Steel Research International*, 9, 1128–1131. <https://doi.org/10.1007/s12289-009-0446-4>
 83. Pinger, T., & Rückriem, E. M. (2016). Investigation on the corrosion and mechanical behavior of thin film batch galvanized thick plate components in clinch joints. *International Journal of Advanced Manufacturing Technology*, 86, 29–36. <https://doi.org/10.1007/s00170-015-8141-8>
 84. Mhawesh, Z. T., Kara, İH., & Zeyveli, M. (2023). Corrosion resistance of interstitial free steel and Mg alloys sheets joined by mechanical clinching. *Journal of Materials Engineering and Performance*, 32, 2793–2800. <https://doi.org/10.1007/s11665-022-07221-5>
 85. Zhang, Y., Xu, H., Peng, R., et al. (2021). Joinability and mechanical properties of clinched joints of different aluminum alloys. *International Journal of Precision Engineering and Manufacturing-Green Technology*, 22, 1883–1896. <https://doi.org/10.1007/s40684-021-00366-z>

Publisher's Note Springer Nature remains neutral with regard to jurisdictional claims in published maps and institutional affiliations.



Jacek Mucha is a professor at Rzeszow University of Technology, Poland, since 2015. He obtained his Ph.D. in mechanical engineering from Faculty of Mechanical Engineering and Aeronautics in 2004, the habilitation in mechanical engineering from Faculty of Mechanical Engineering and Aeronautics in 2014. His research interests are focused on metal forming, joining by plastic deformation and mechanical design, FEM analysis, mainly studying self-piercing riveting connection technology

and resistance spot welding connection technology, and clinching technology of thin sheet materials.



Łukasz Boda received his master's degree in Rzeszów University of Technology at the Faculty of Mechanical Engineering and Aeronautics. In 2020, he joined the Doctoral School of the Rzeszów University of Technology. He is participant of the research group for clinching and clinch-rivet technologies. Simultaneously attends doctoral school and work in industry as designer-technologist of the injection mold manufacturer.



Waldemar Witkowski received his M.Sc. (2010) and Ph.D. Eng. (2017) from the Faculty of Mechanical Engineering and Aeronautics at Rzeszów University of Technology in Poland. He is currently an associate professor in the Department of Mechanical Engineering at Rzeszów University of Technology. His research interest is mechanical design, FEM analysis, joining technologies of thin-walled structures, bearing lubrication.